Electronic Supplementary Material (ESI) for Physical Chemistry Chemical Physics

Supporting Information

Lowest excited states and optical absorption spectra of donor-acceptor copolymers for organic photovoltaics: A new picture emerging from tuned long-range corrected density functionals

Laxman Pandey, Curtis Doiron, John S. Sears, and Jean-Luc Brédas[*,¥]*

School of Chemistry & Biochemistry and Center for Organic Photonics and Electronics

Georgia Institute of Technology

Atlanta, Georgia 30332-0400

* Email: jean-luc.bredas@chemistry.gatech.edu

[¥] Also affiliated with: Department of Chemistry, King Abdulaziz University, Jeddah 21589, Saudi Arabia

Table S1. Tuned omega values ($bohr^{-1}$) for the ωB97 and BNL functionals from monomer to hexamer.

n	1	2	3	4	5	6
ωB97						
PBDTTPD	0.188	0.144	0.129	0.124	0.122	0.124
PBDTTT-C	0.190	0.141	0.124	0.117	0.114	0.115
PBDTTT-CF	0.188	0.142	0.125	0.118	0.115	0.116
PBDTTT-E	0.185	0.139	0.123	0.115	0.119	0.116
PCDTBT	0.186	0.156	0.151	0.152		
PCPDTBT	0.197	0.152	0.125	0.113	0.107	0.104
BNL						
PBDTTPD	0.196	0.150	0.134	0.129		
PBDTTT-C	0.197	0.147	0.129	0.121		
PBDTTT-CF	0.196	0.148	0.130	0.123		
PBDTTT-E	0.193	0.144	0.127	0.120		
PCDTBT	0.194	0.162	0.158	0.158		
PCPDTBT	0.211	0.160	0.132	0119		

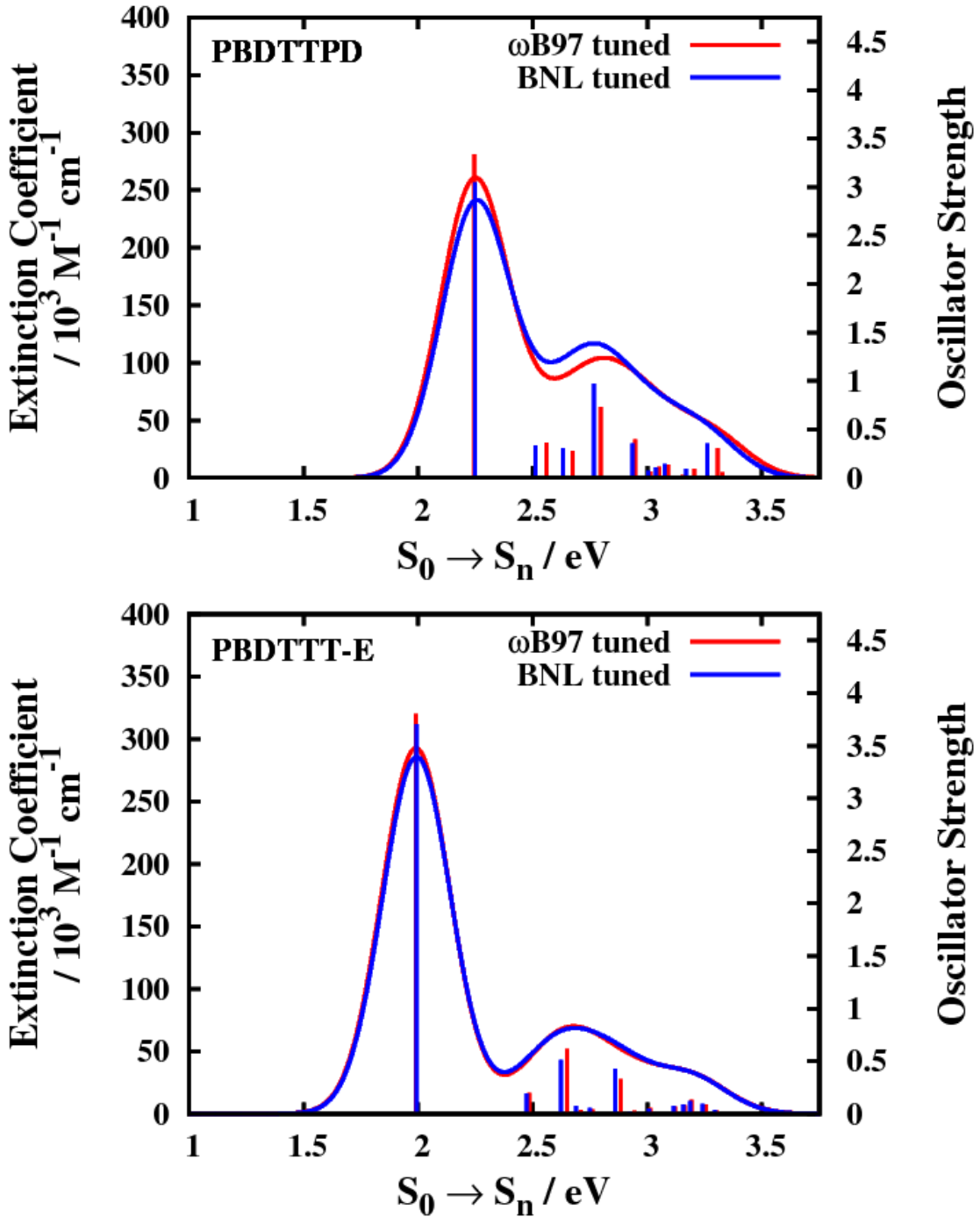

Figure S1 (a). Calculated optical absorption spectra from tuned ωB97 and BNL for the tetramers of PBDTTPD and PBDTTT-E at the TD-DFT level.

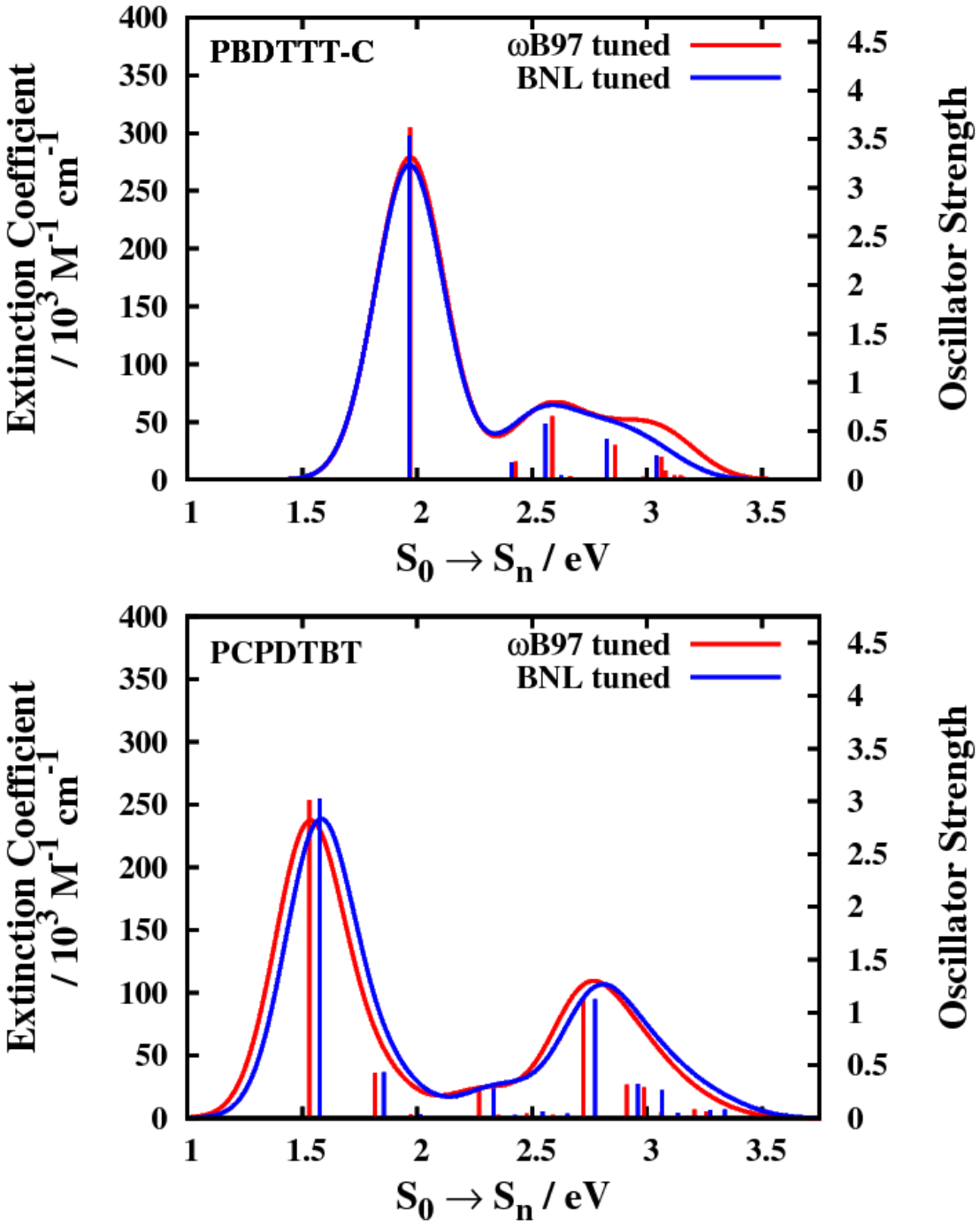

Figure S1 (b). Calculated optical absorption spectra from tuned ωB97 and BNL for the tetramers of PBDTTT-C and PCPDTBT at the TD-DFT level.

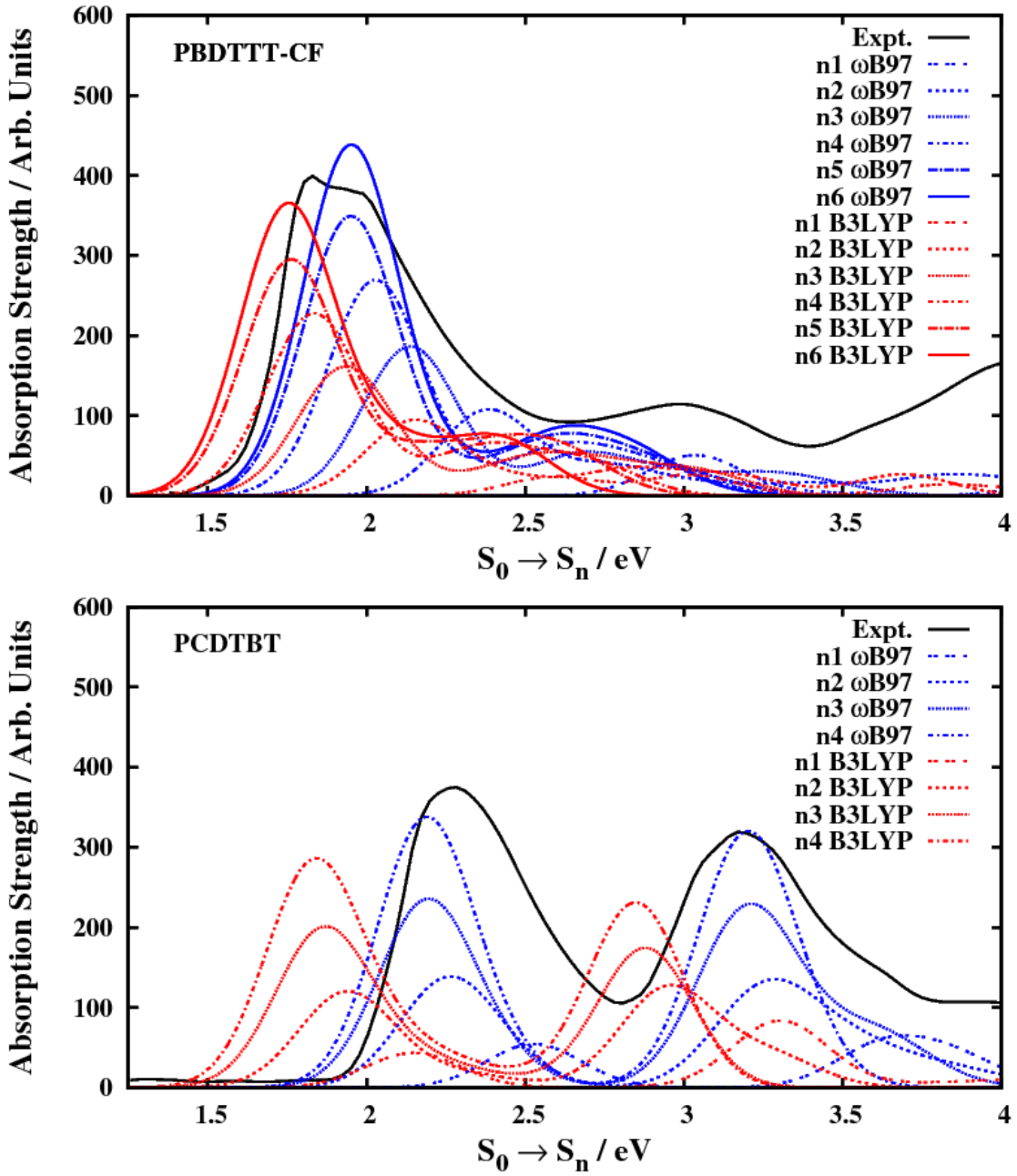

Figure S2 (a). Calculated optical absorption spectra from tuned ωB97 and from B3LYP for varying lengths of oligomers compared to the digitized experimental data: PBDTTT-CF [1] and PCDTBT.[2]

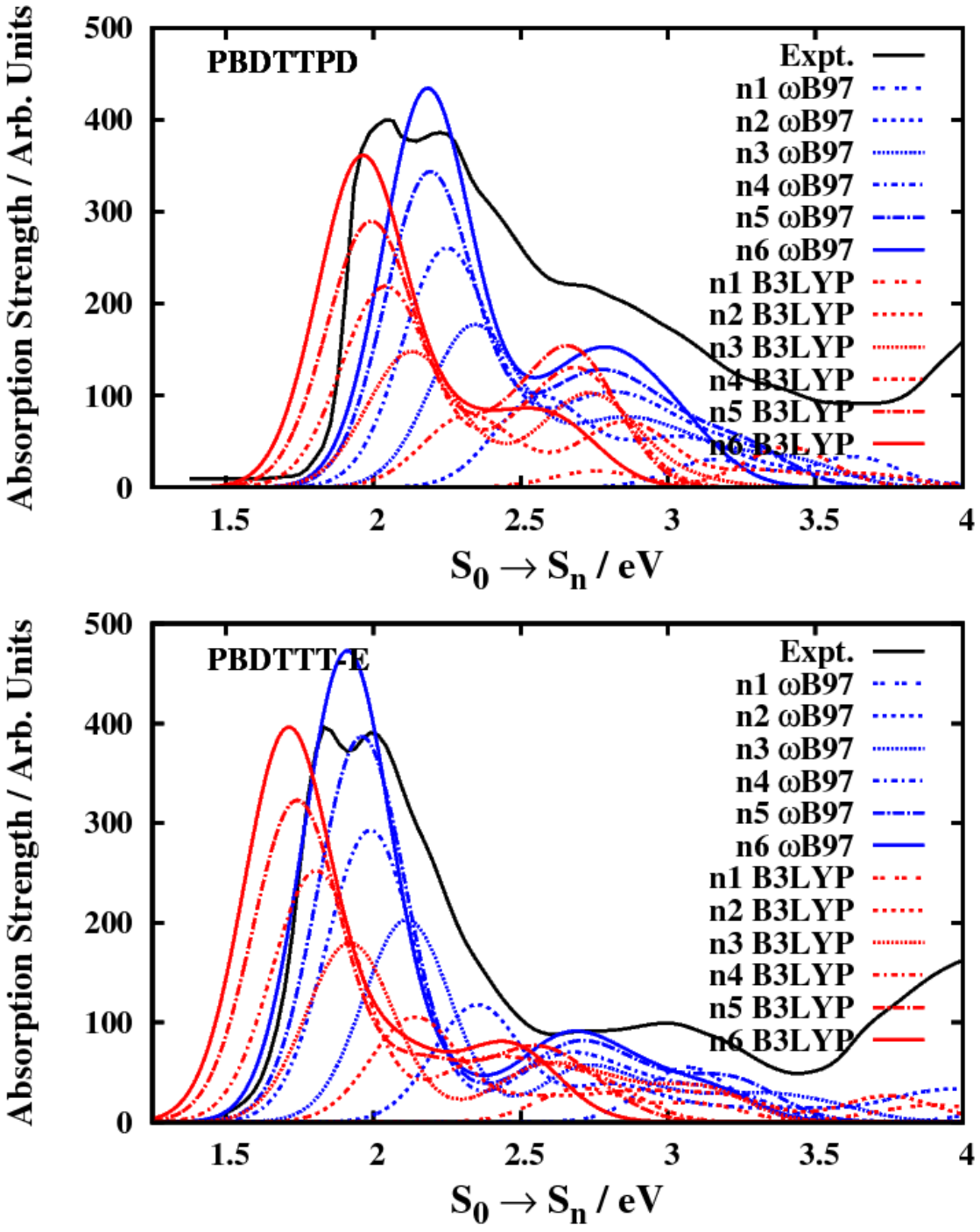

Figure S2 (b). Calculated optical absorption spectra from tuned ωB97 and from B3LYP for varying lengths of oligomers compared to the digitized experimental data: PBDTTPD [3] and PBDTTT-E.[1]

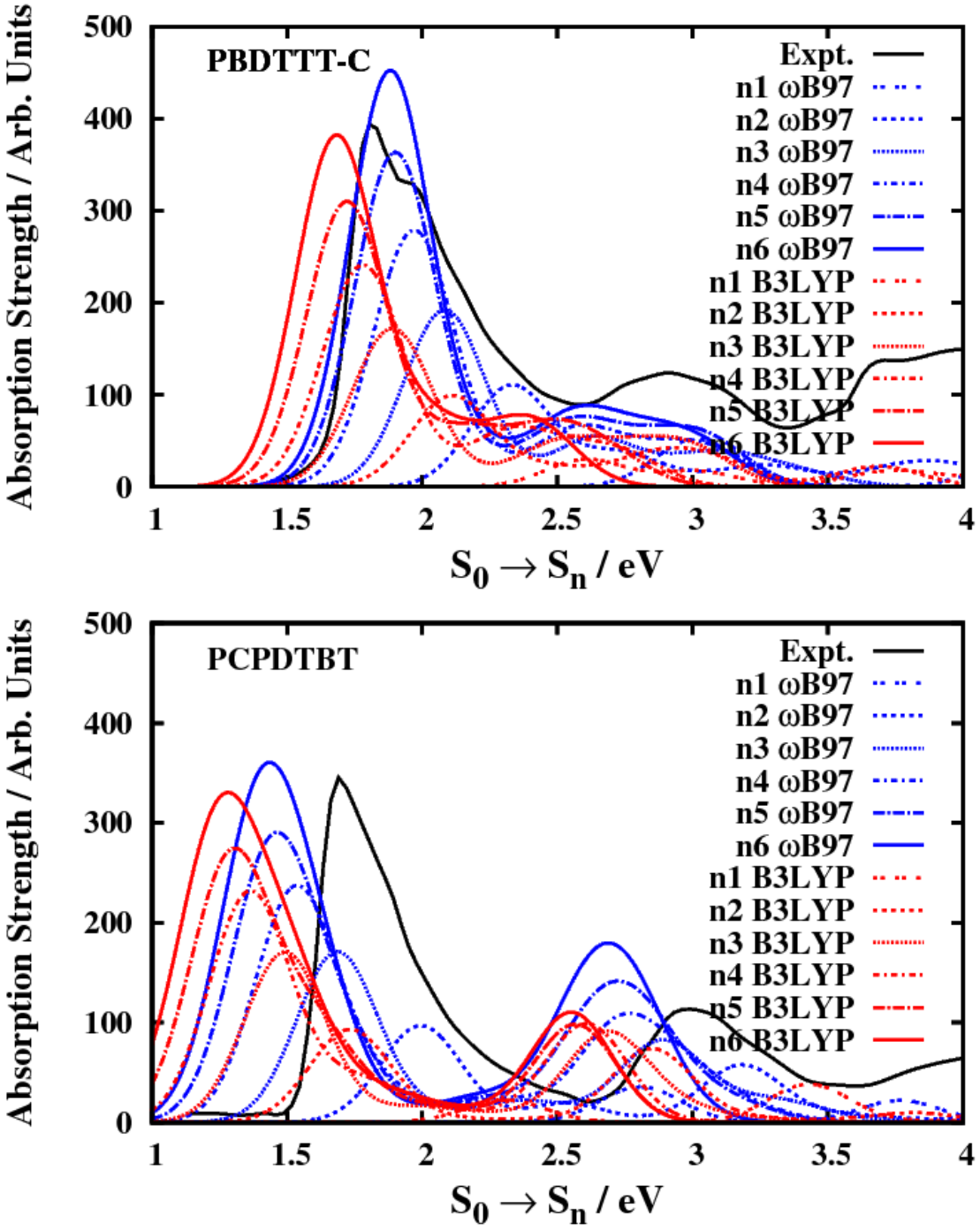

Figure S2 (c). Calculated optical absorption spectra from tuned ωB97 and from B3LYP for varying lengths of oligomers compared to the digitized experimental data: PBDTTT-C [1] and PCPDTBT.[4]

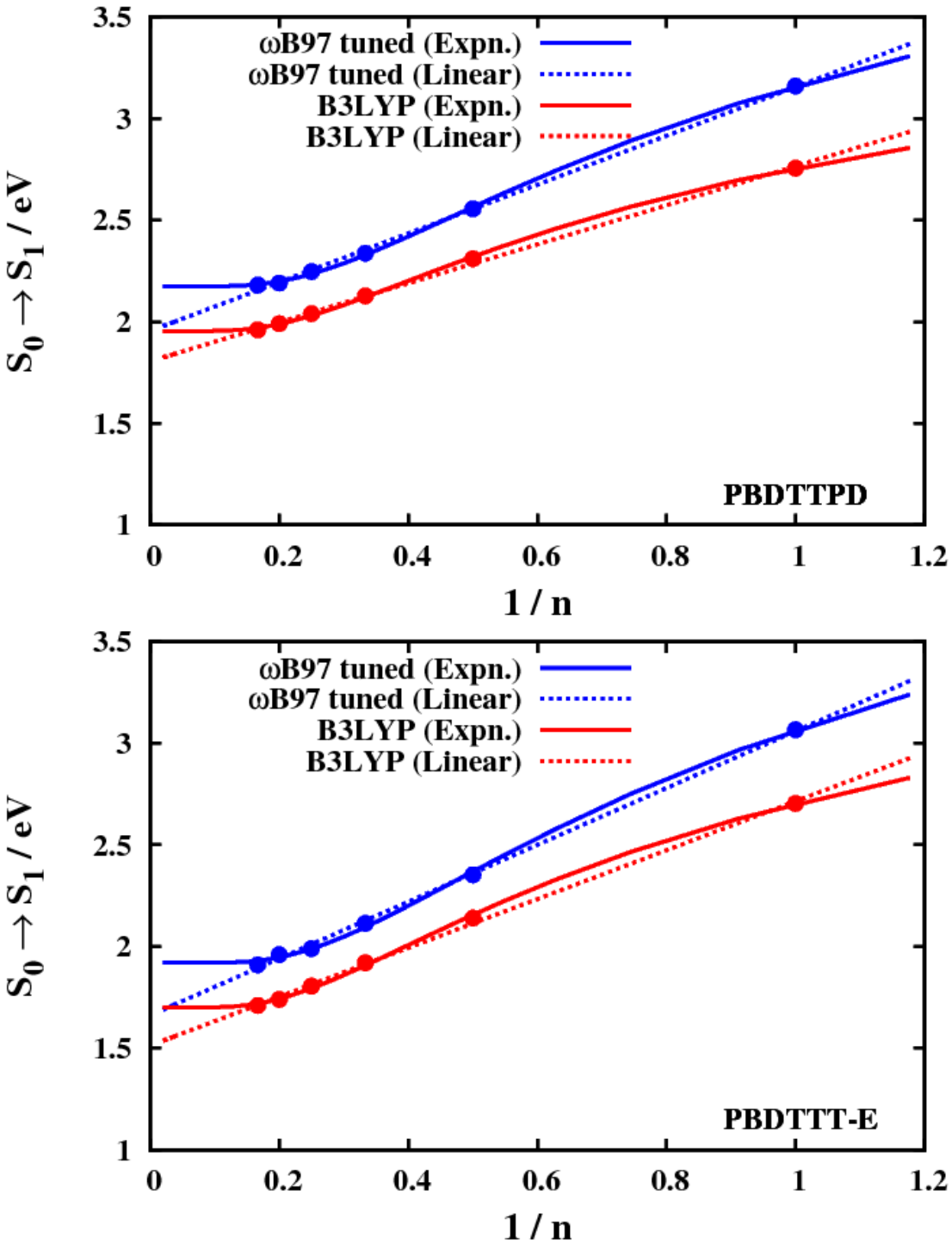

Figure S3 (a). Evolution of the first transition energy ($S_0 \rightarrow S_1$) with respect to inverse number of repeat units (1/n) for PBDTTPD and PBDTTT-E at the TD-DFT level for the B3LYP and tuned ωB97 functionals. Extrapolations of the $S_0 \rightarrow S_1$ energy using linear and exponential [5] fits are also included.

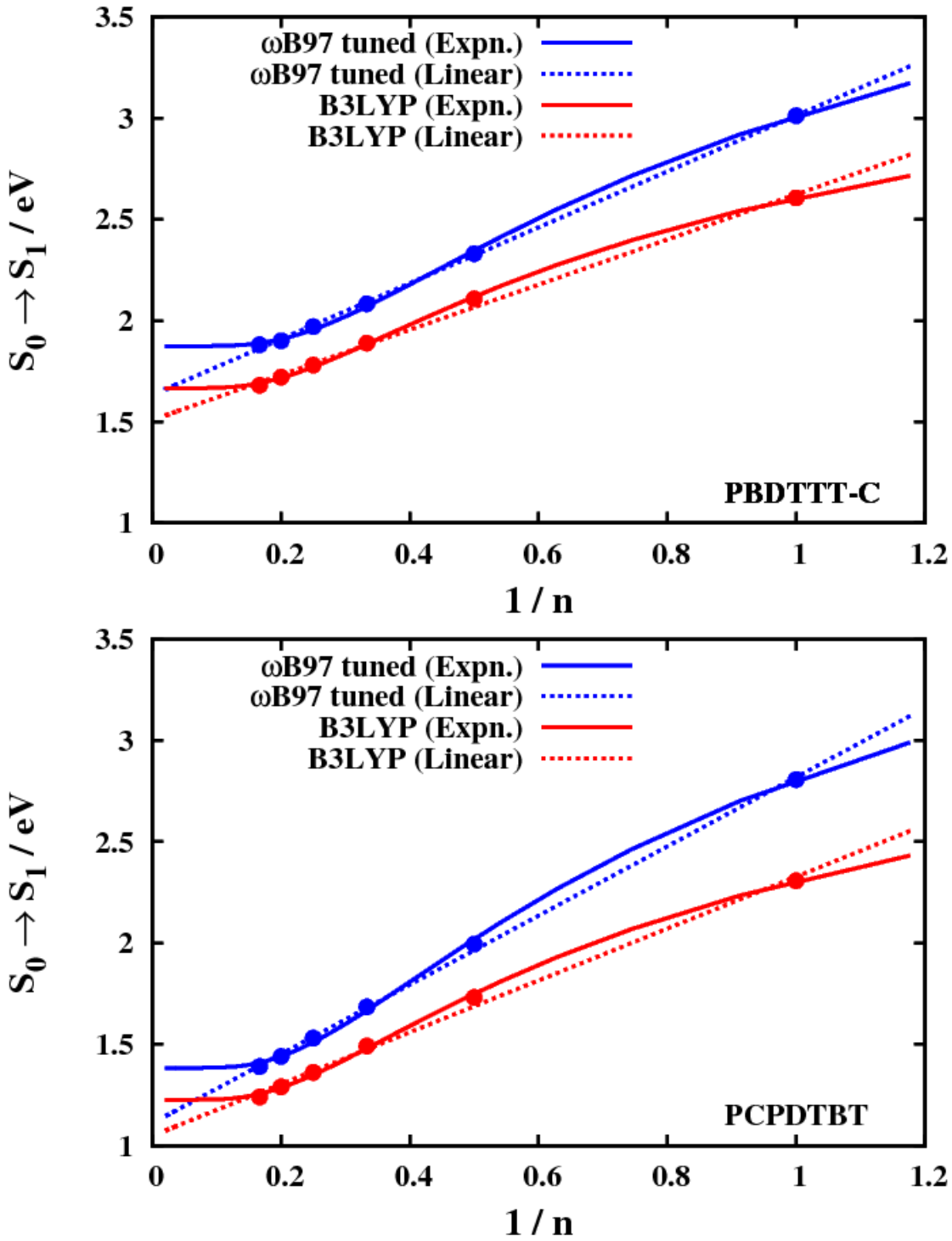

Figure S3 (b). Evolution of the first transition energy ($S_0 \rightarrow S_1$) with respect to inverse number of repeat units (1/n) for PBDTTT-C and PCPDTBT at the TD-DFT level for the B3LYP and tuned ωB97 functionals. Extrapolations of the $S_0 \rightarrow S_1$ energy using linear and exponential [5] fits are also included.

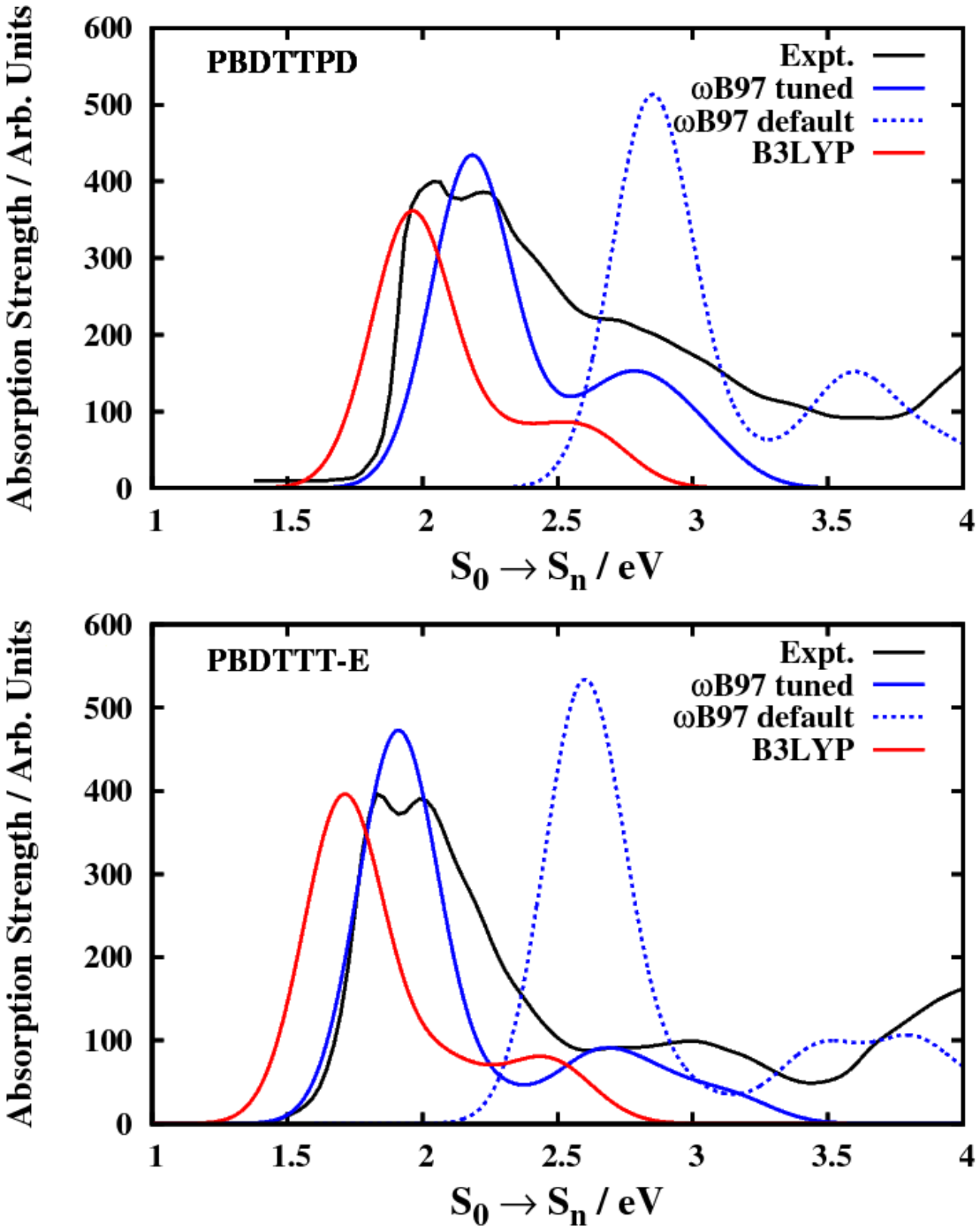

Figure S4 (a). Calculated optical absorption spectra from ωB97 (default and tuned ω) and B3LYP for the isolated hexamers of PBDTTPD and PBDTTT-E compared to the digitized experimental data.

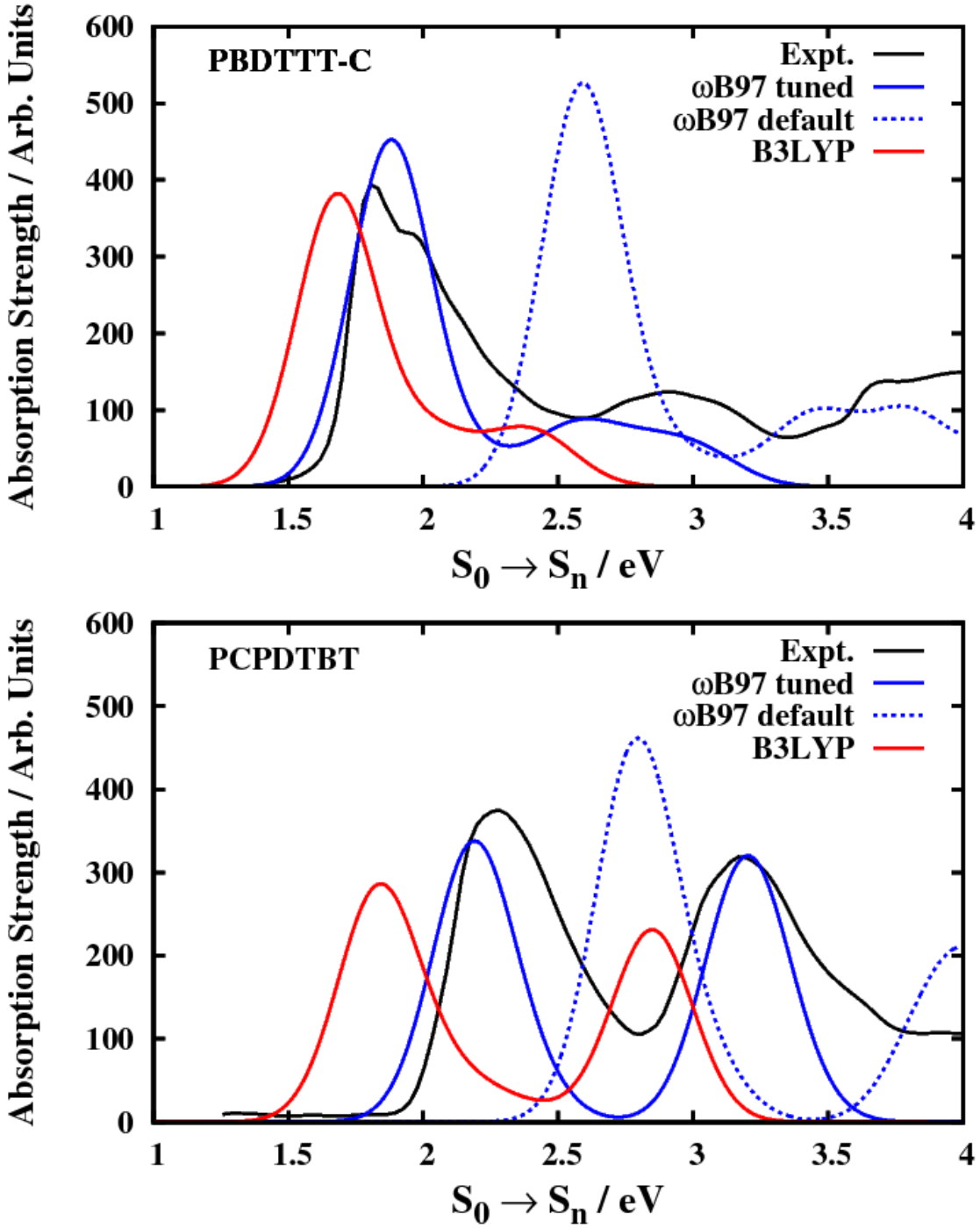

Figure S4 (b). Calculated optical absorption spectra from ωB97 (default and tuned ω) and B3LYP for the isolated hexamers of PBDTTT-C and PCPDTBT compared to the digitized experimental data.

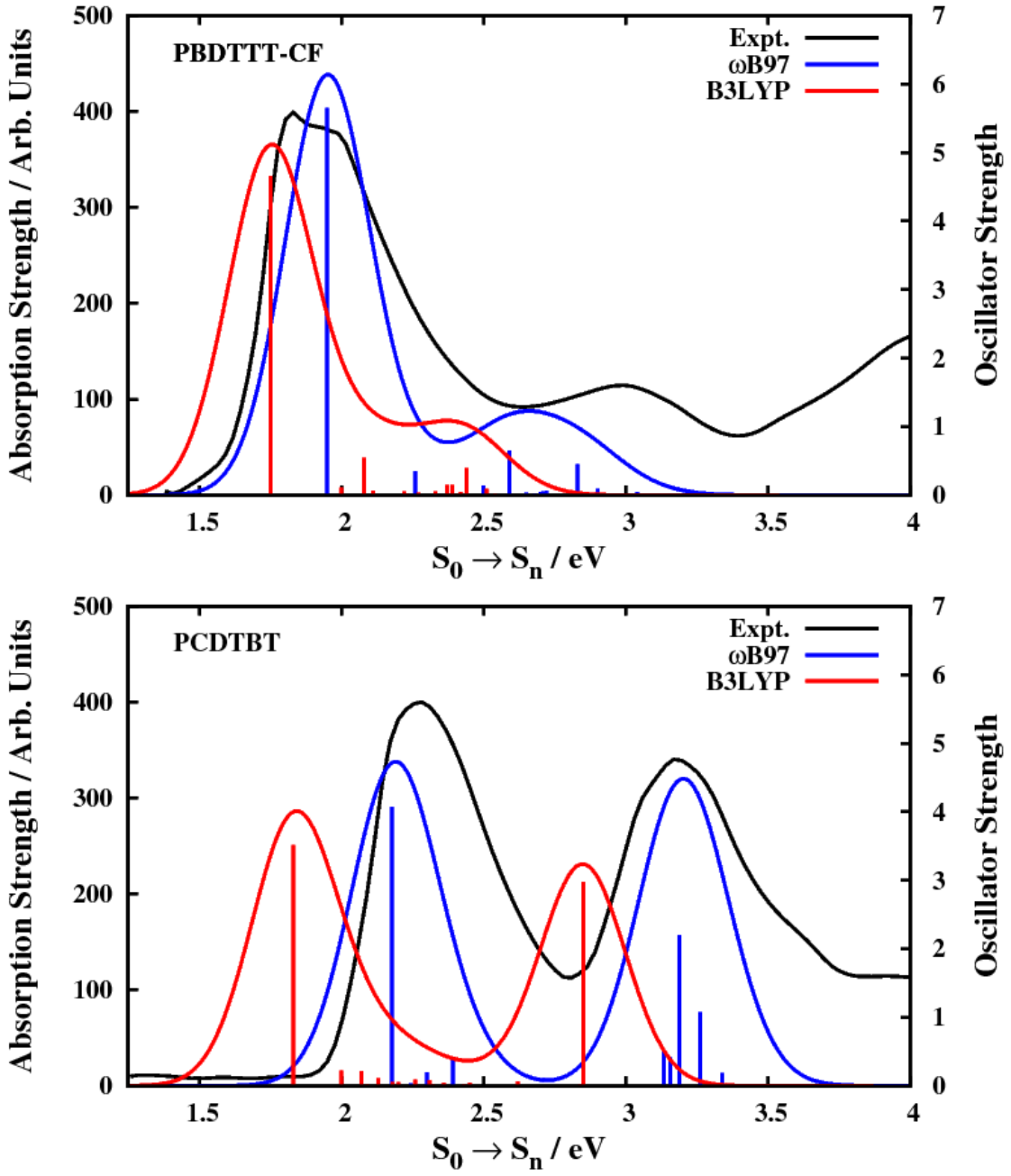

Figure S5 (a). Calculated optical absorption spectra from tuned ωB97 and from B3LYP for isolated hexamer of PBDTTT-CF and tetramer of PCDTBT, compared to the digitized experimental data.

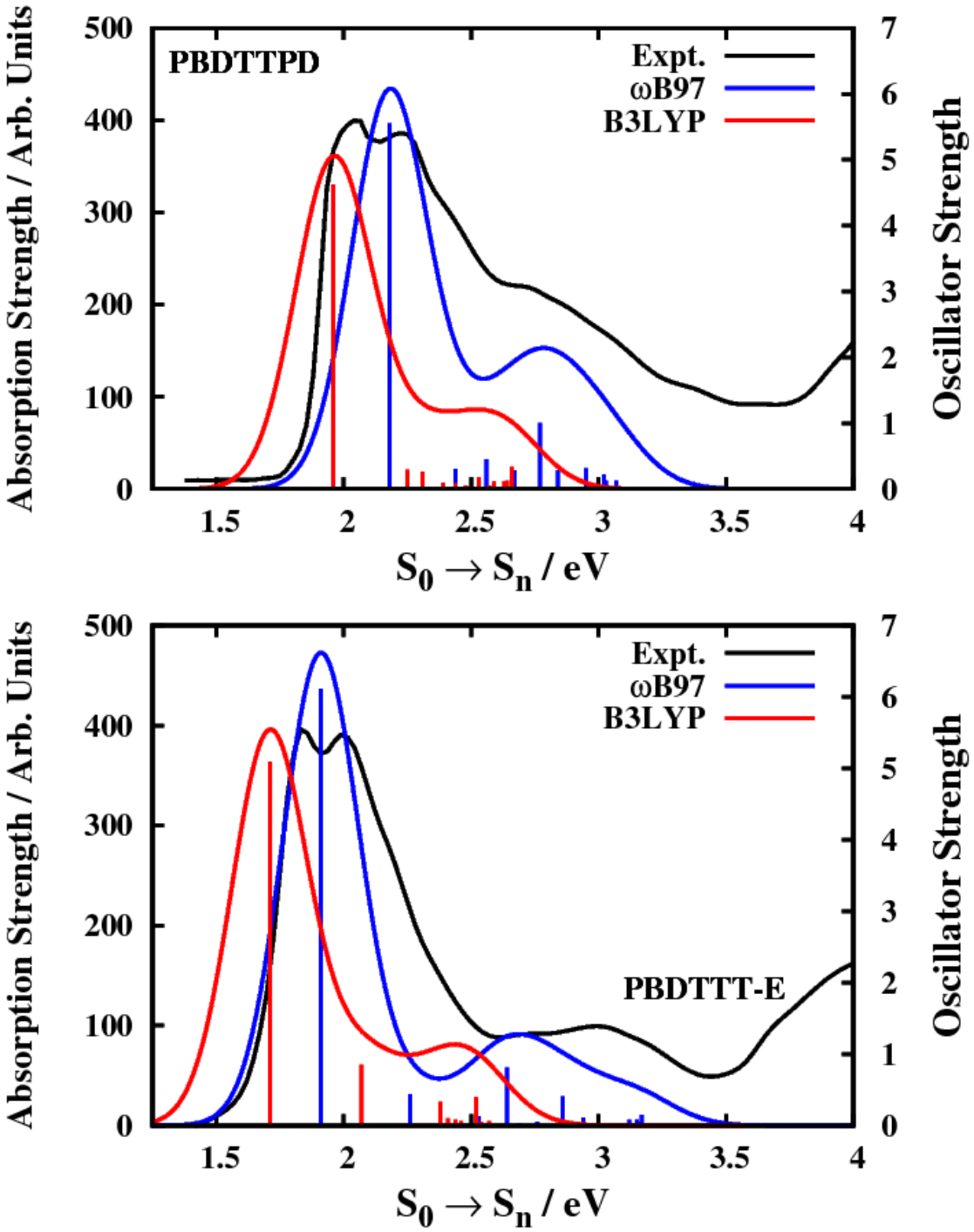

Figure S5 (b). Calculated optical absorption spectra from tuned ωB97 and from B3LYP for isolated hexamers of PBDTTPD and PBDTTT-E compared to the digitized experimental data.

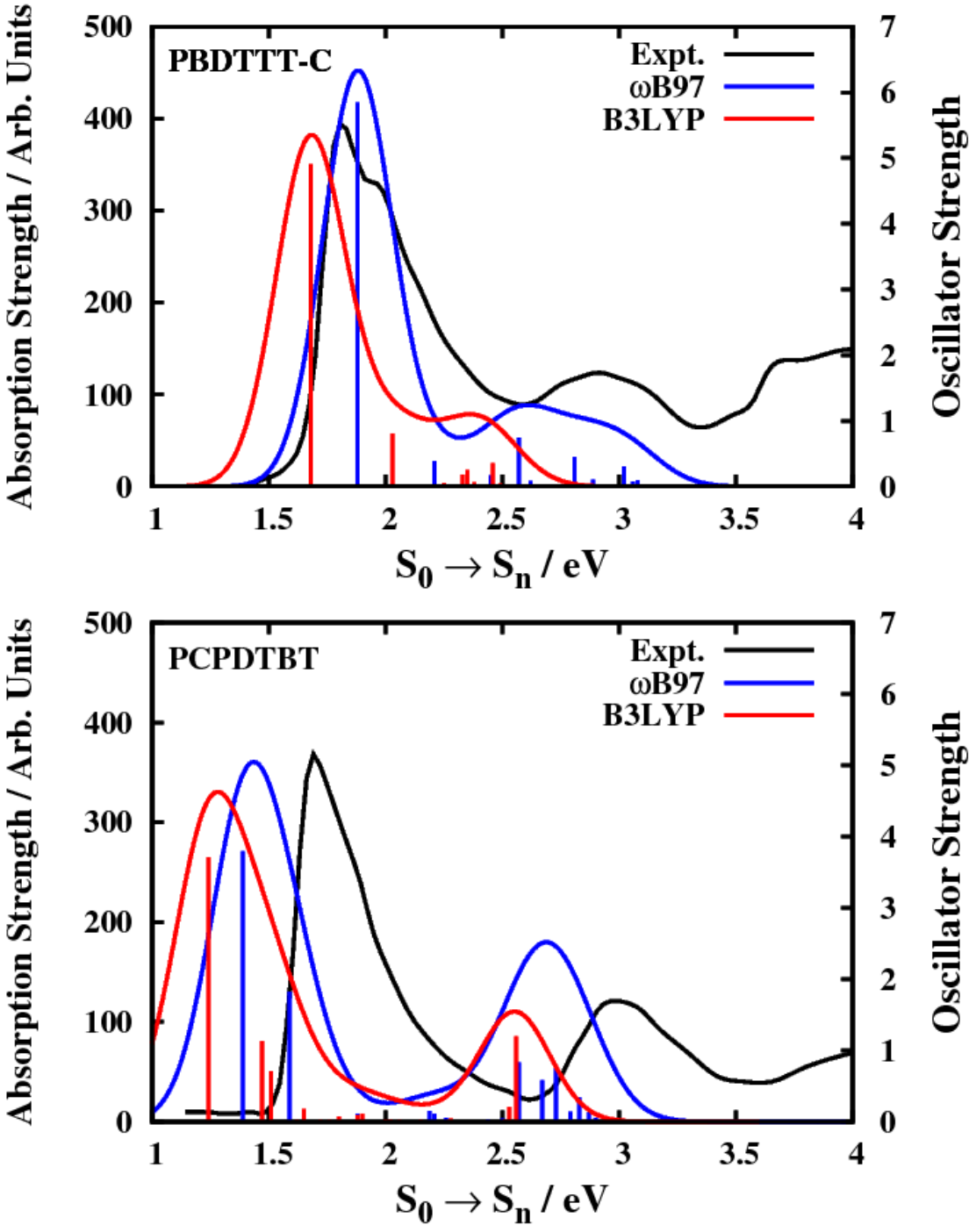

Figure S5 (c). Calculated optical absorption spectra from tuned ωB97 and from B3LYP for isolated hexamers of PBDTTT-C and PCPDTBT compared to the digitized experimental data.

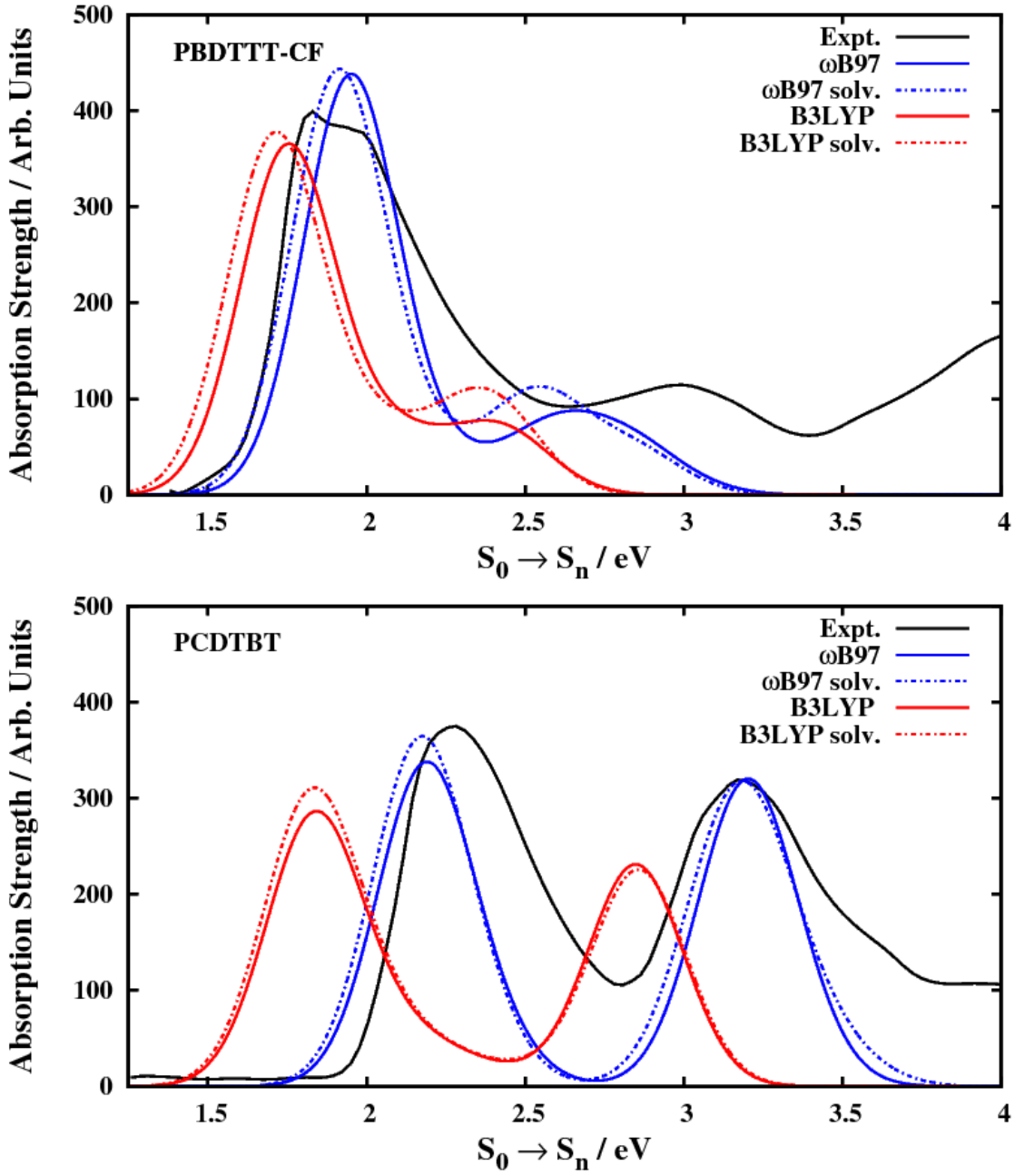

Figure S6 (a). Calculated gas-phase and solvent environment optical absorption spectra from tuned ωB97 and from B3LYP for the hexamer of PBDTTT-CF and tetramer of PCDTBT, compared to the digitized experimental data.

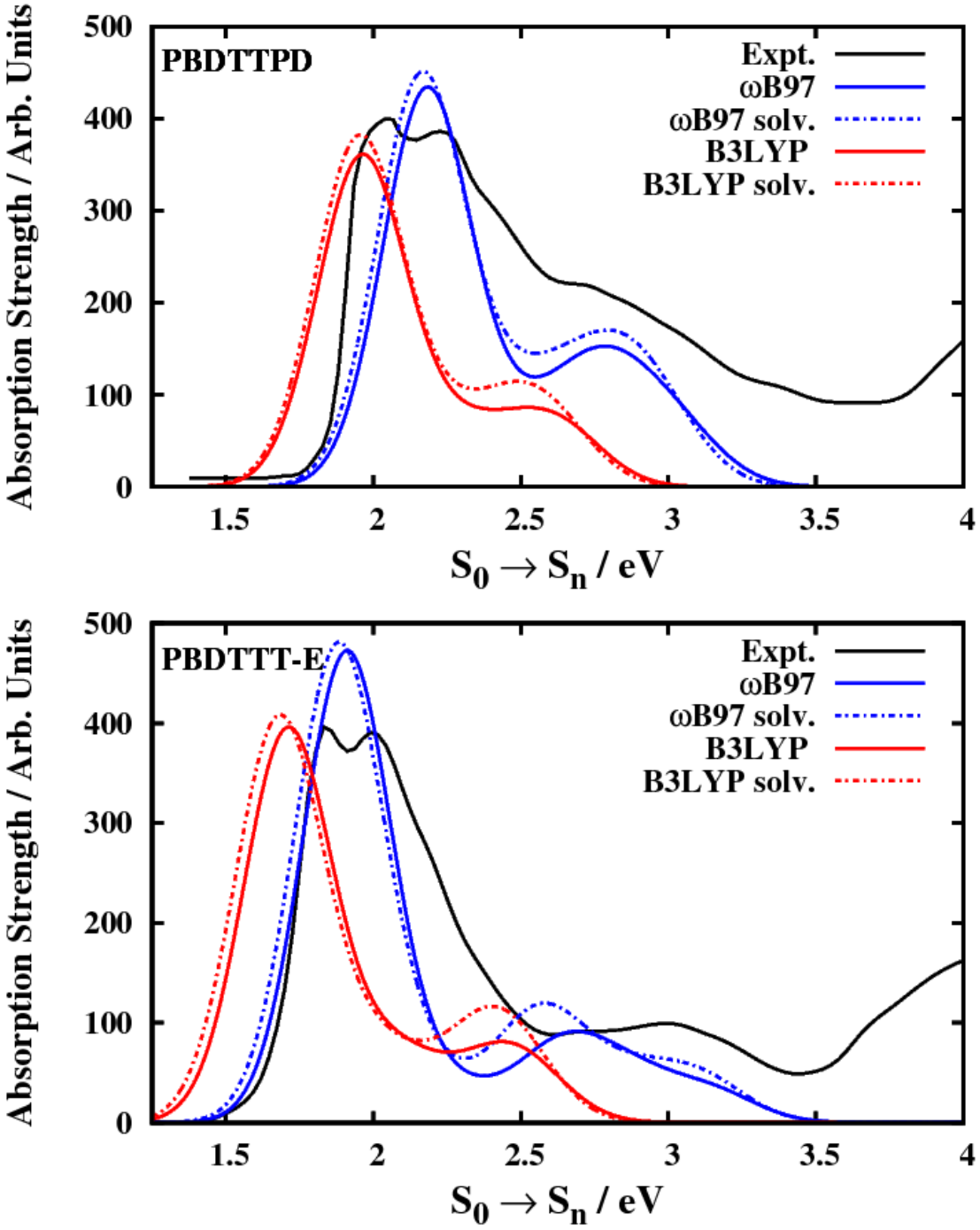

Figure S6 (b). Calculated gas-phase and solvent environment optical absorption spectra from tuned ωB97 and from B3LYP for the hexamers of PBDTTPD and PBDTTT-E compared to the digitized experimental data.

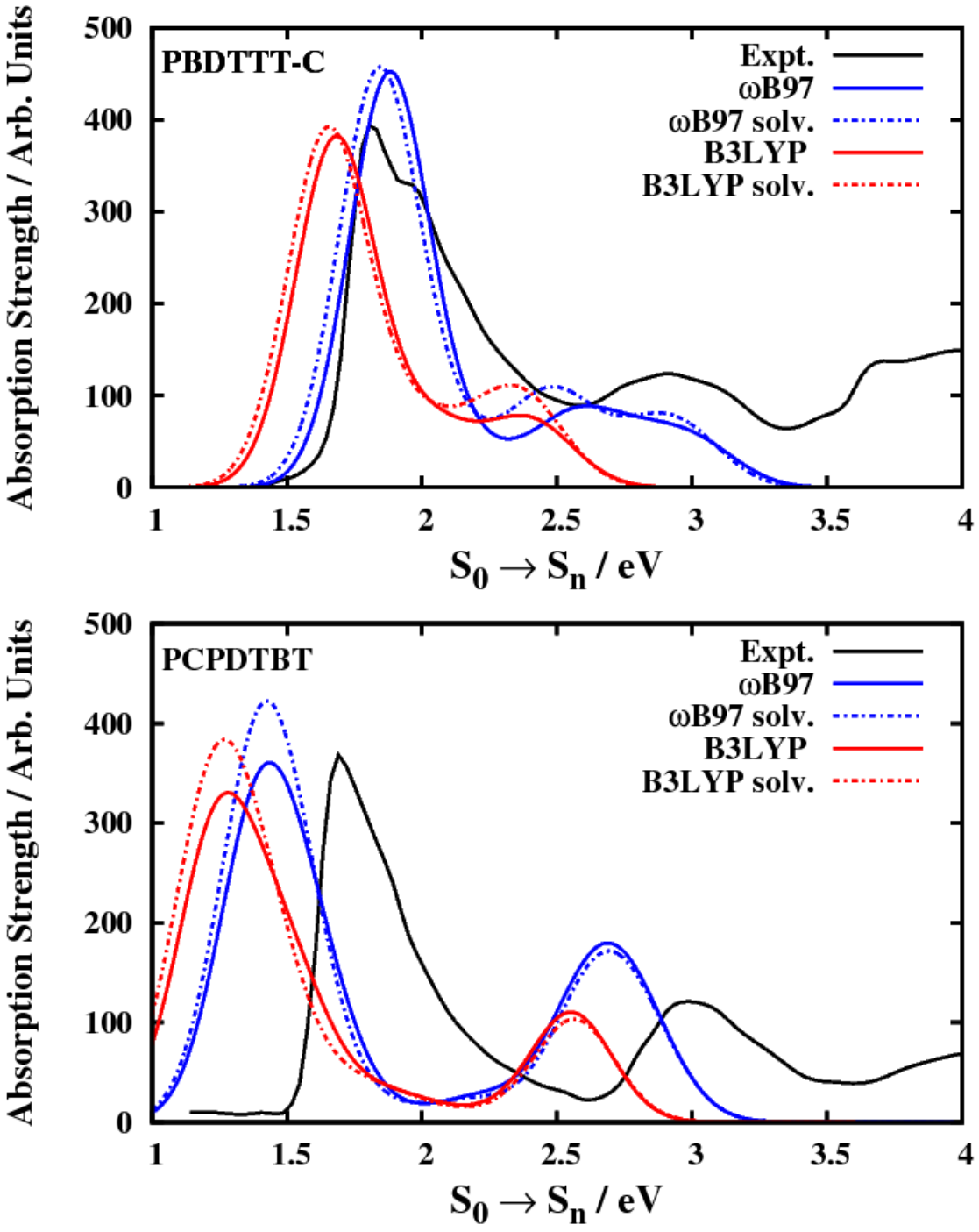

Figure S6 (c). Calculated gas-phase and solvent environment optical absorption spectra from tuned ωB97 and from B3LYP for the hexamers of PBDTTT-C and PCPDTBT compared to the digitized experimental data.

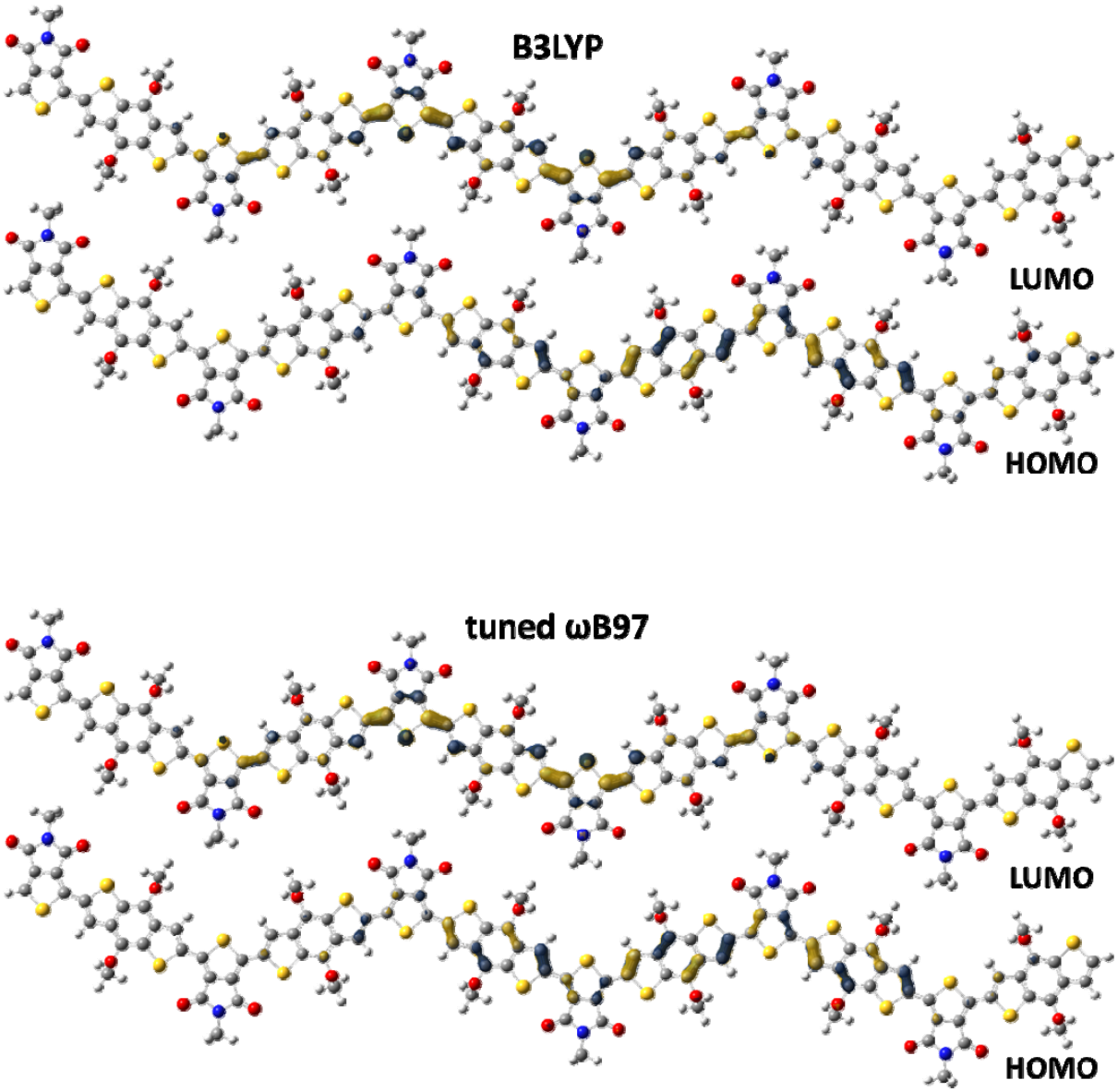

Figure S7. Illustration of the qualitatively similar HOMO and LUMO wave functions (isovalue surface 0.03 a.u.in the hexamer of PBDTTPD for B3LYP and tuned ωB97.

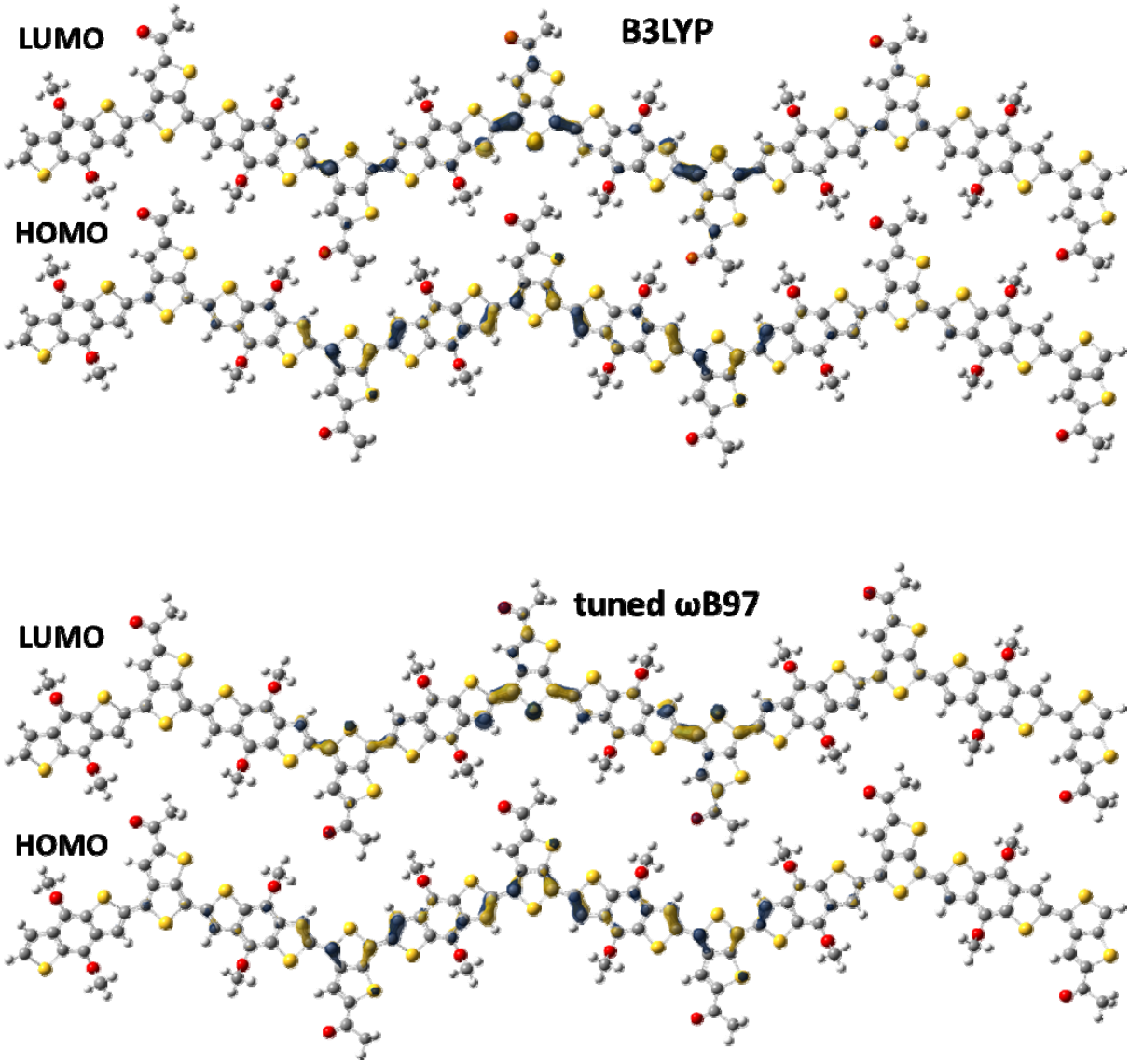

Figure S8. Illustration of the qualitatively similar HOMO and LUMO wave functions (isovalue surface 0.03 a.u.) in the hexamer of PBDTTT-C for B3LYP and tuned ωB97.

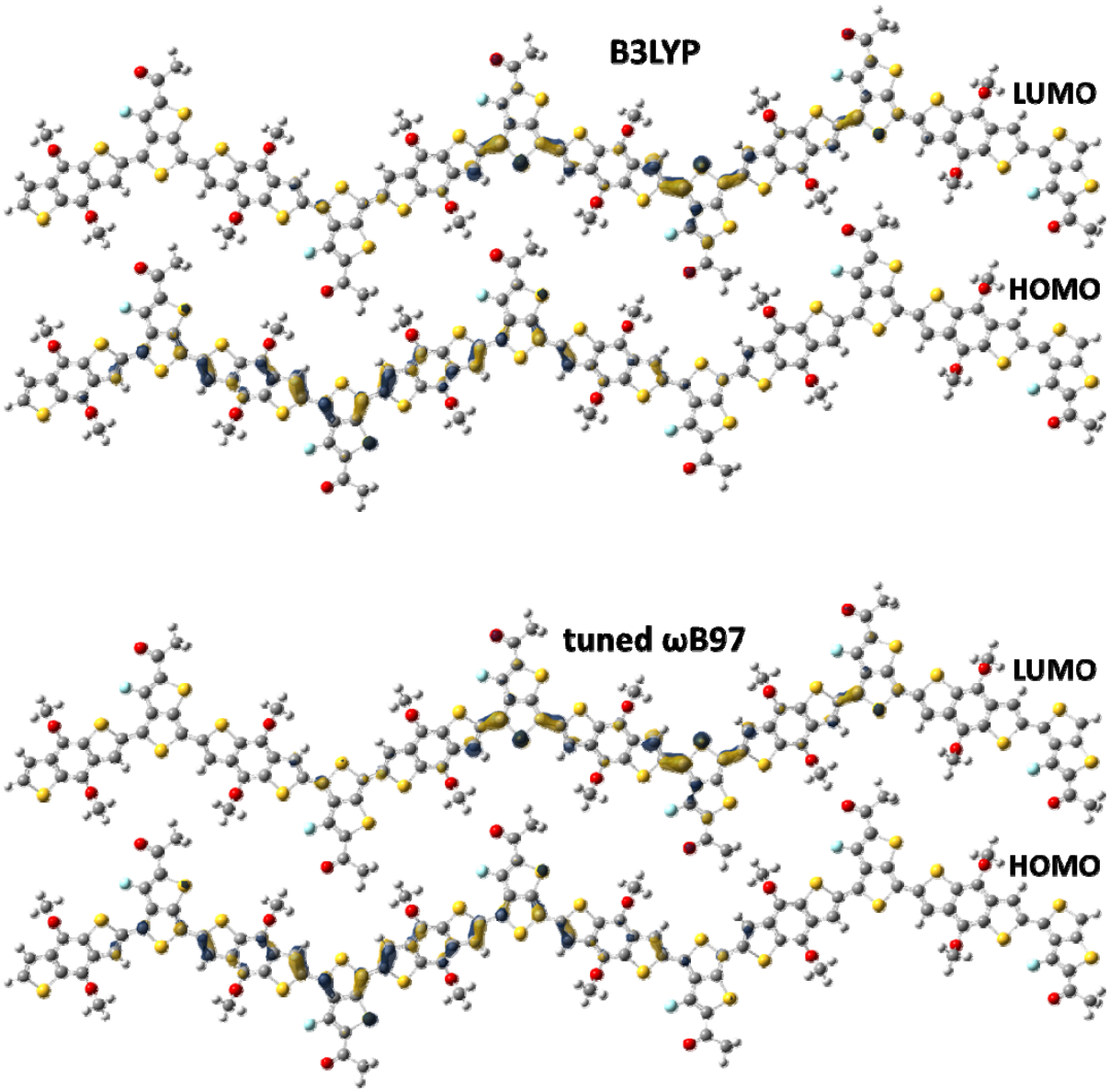

Figure S9. Illustration of the qualitatively similar HOMO and LUMO wave functions (isovalue surface 0.03 a.u.) in the hexamer of PBDTTT-CF for B3LYP and tuned ωB97.

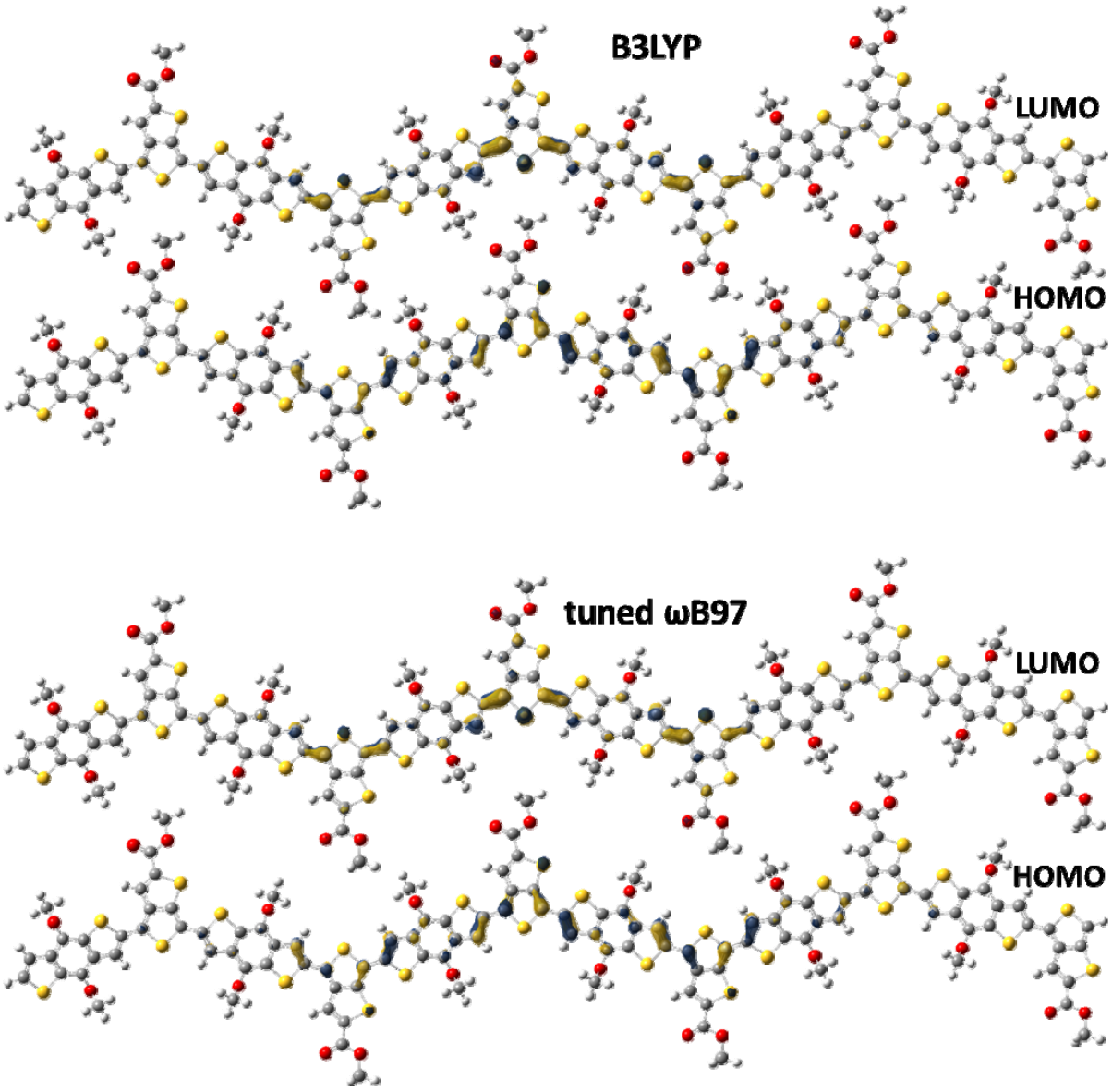

Figure S10. Illustration of the qualitatively similar HOMO and LUMO wave functions (isovalue surface 0.03 a.u.) in the hexamer of PBDTTT-E for B3LYP and tuned ωB97.

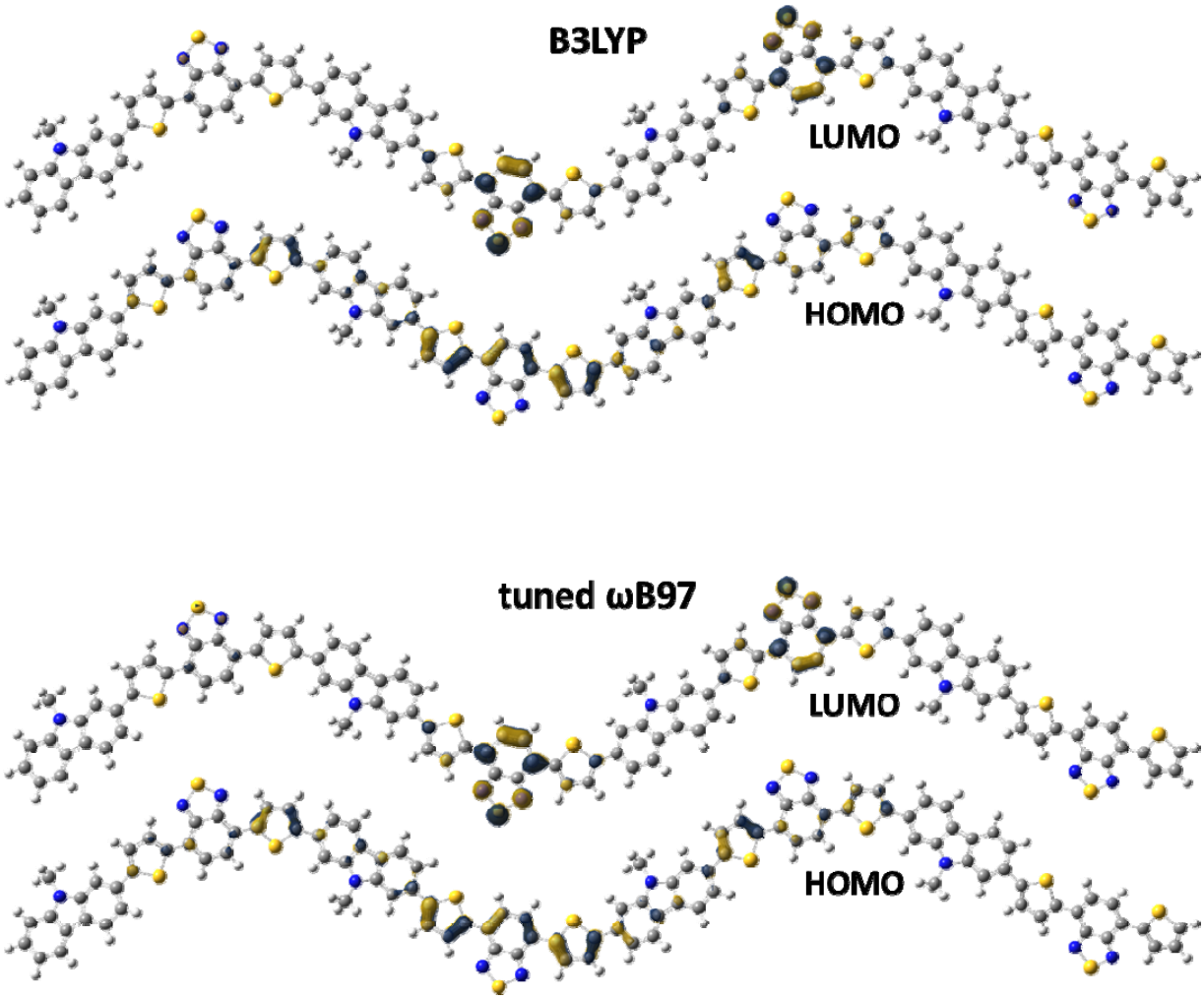

Figure S11. Illustration of the qualitatively similar HOMO and LUMO wave functions (isovalue surface 0.03 a.u.) in the tetramer of PCDTBT for B3LYP and tuned ωB97.

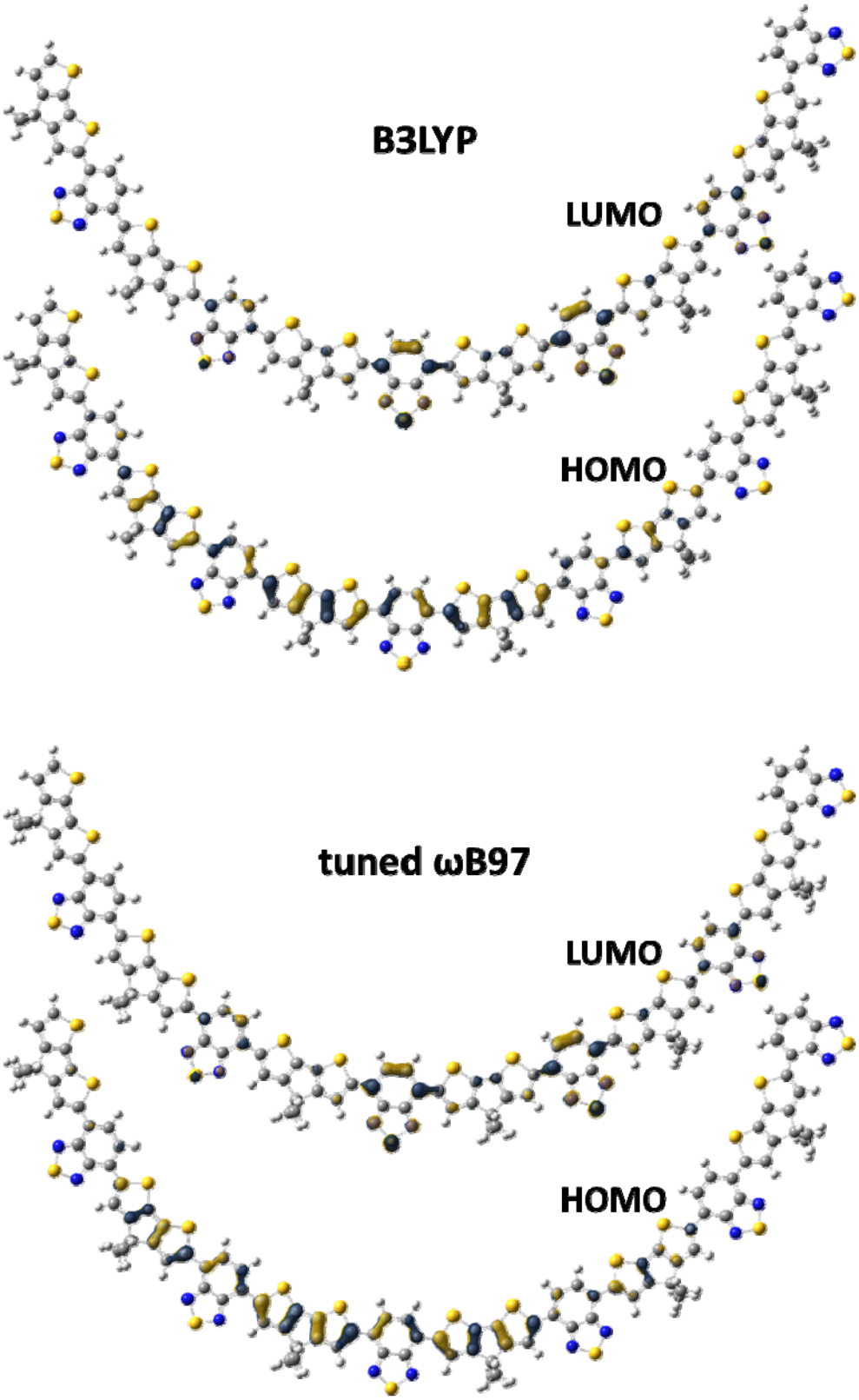

Figure S12. Illustration of the qualitatively similar HOMO and LUMO wave functions (isovalue surface 0.03 a.u.) in the hexamer of PCPDTBT for B3LYP and tuned ωB97.

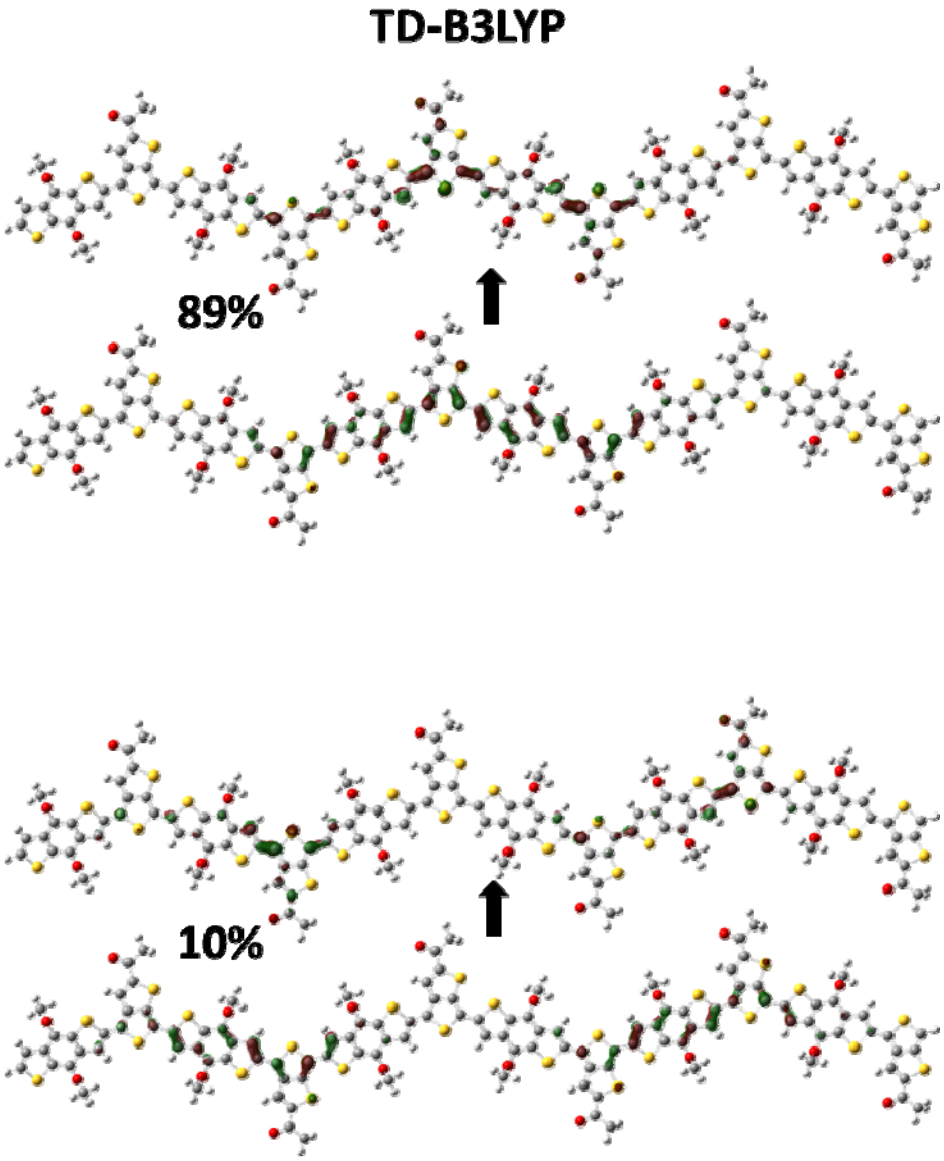

Figure S13 (a). Natural transition orbitals (isovalue surface 0.03 a.u.) for the $S_0 \rightarrow S_1$ excitation in the hexamer of PBDTTT-C at the TD-DFT level for B3LYP. Weights of the hole-particle contribution to the excitation also included.

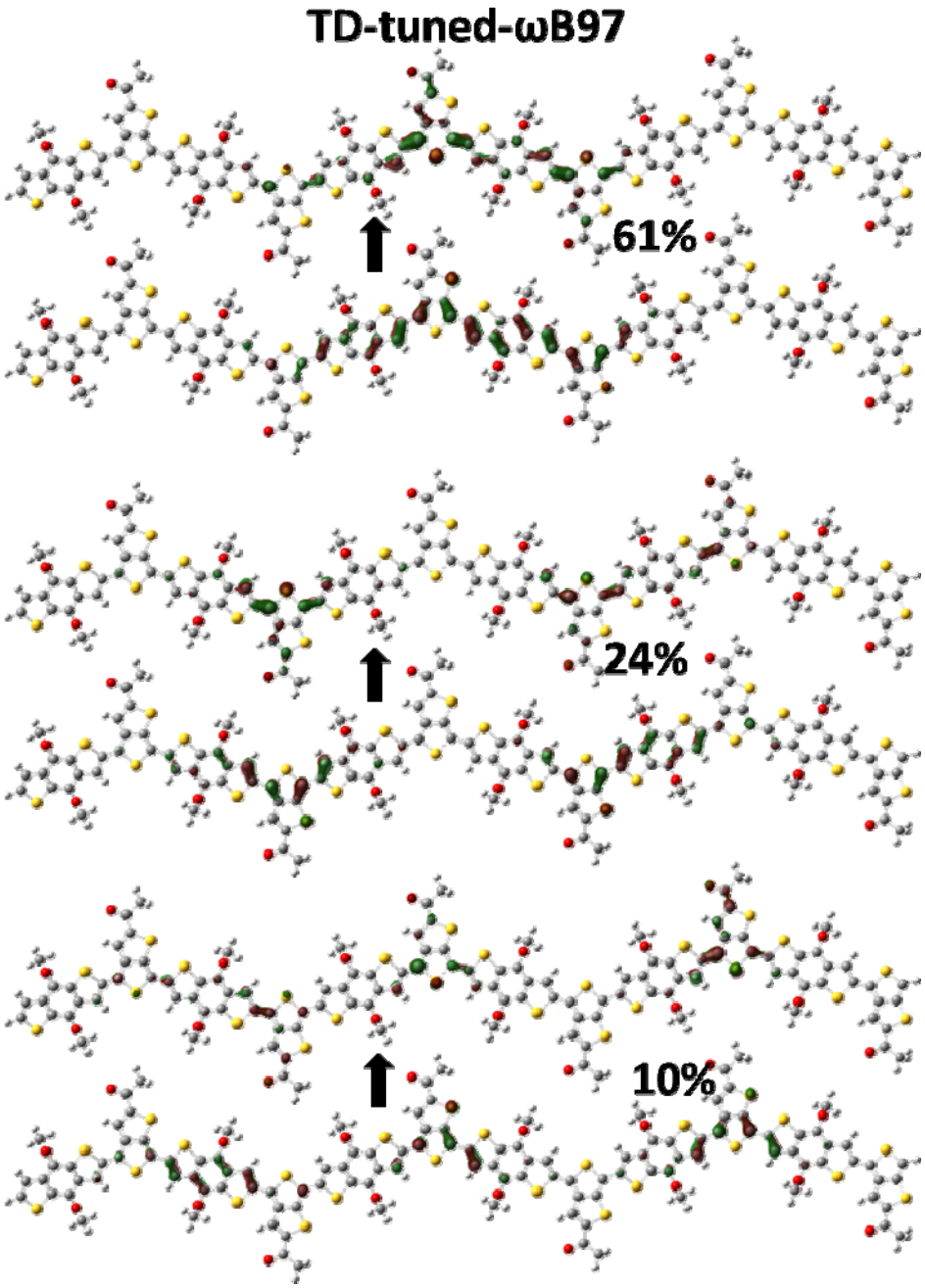

Figure S13 (b). Natural transition orbitals (isovalue surface 0.03 a.u.) for the $S_0 \rightarrow S_1$ excitation in the hexamer of PBDTTT-C at the TD-DFT level for tuned ωB97. Weights of the hole-particle contribution to the excitation also included.

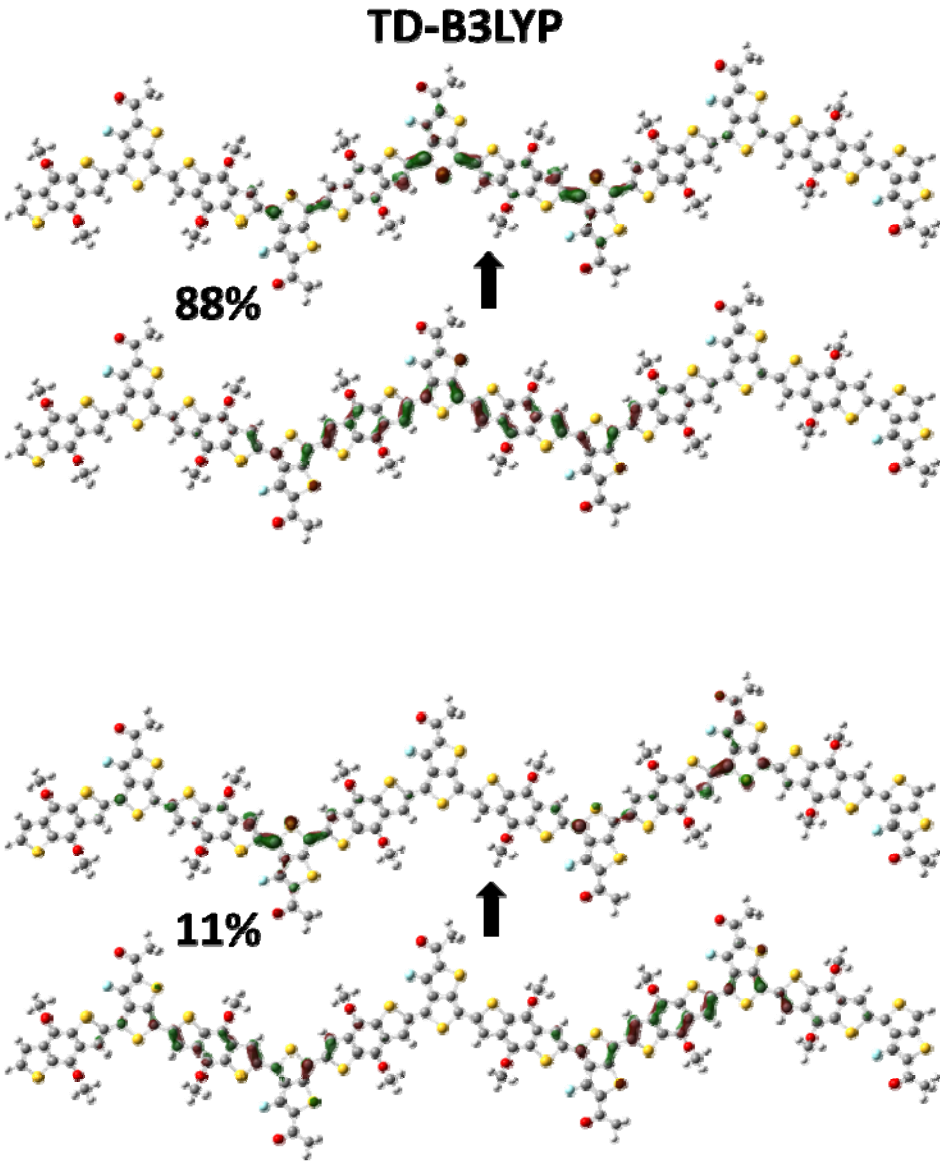

Figure S14 (a). Natural transition orbitals (isovalue surface 0.03 a.u.) for the $S_0 \rightarrow S_1$ excitation in the hexamer of PBDTTT-CF at the TD-DFT level for B3LYP. Weights of the hole-particle contribution to the excitation also included.

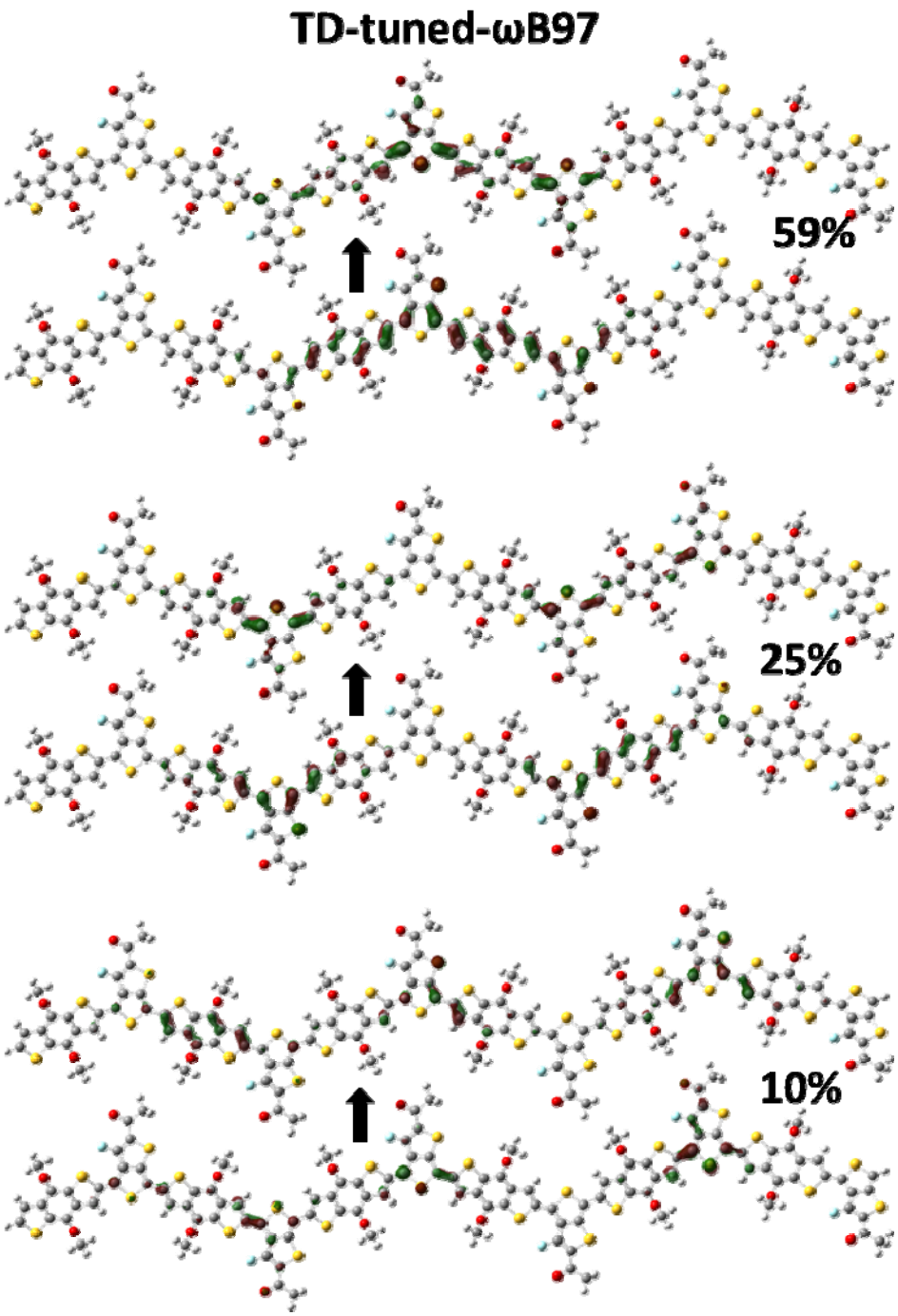

Figure S14 (b). Natural transition orbitals (isovalue surface 0.03 a.u.) for the $S_0 \rightarrow S_1$ excitation in the hexamer of PBDTTT-CF at the TD-DFT level for tuned ωB97. Weights of the hole-particle contribution to the excitation also included.

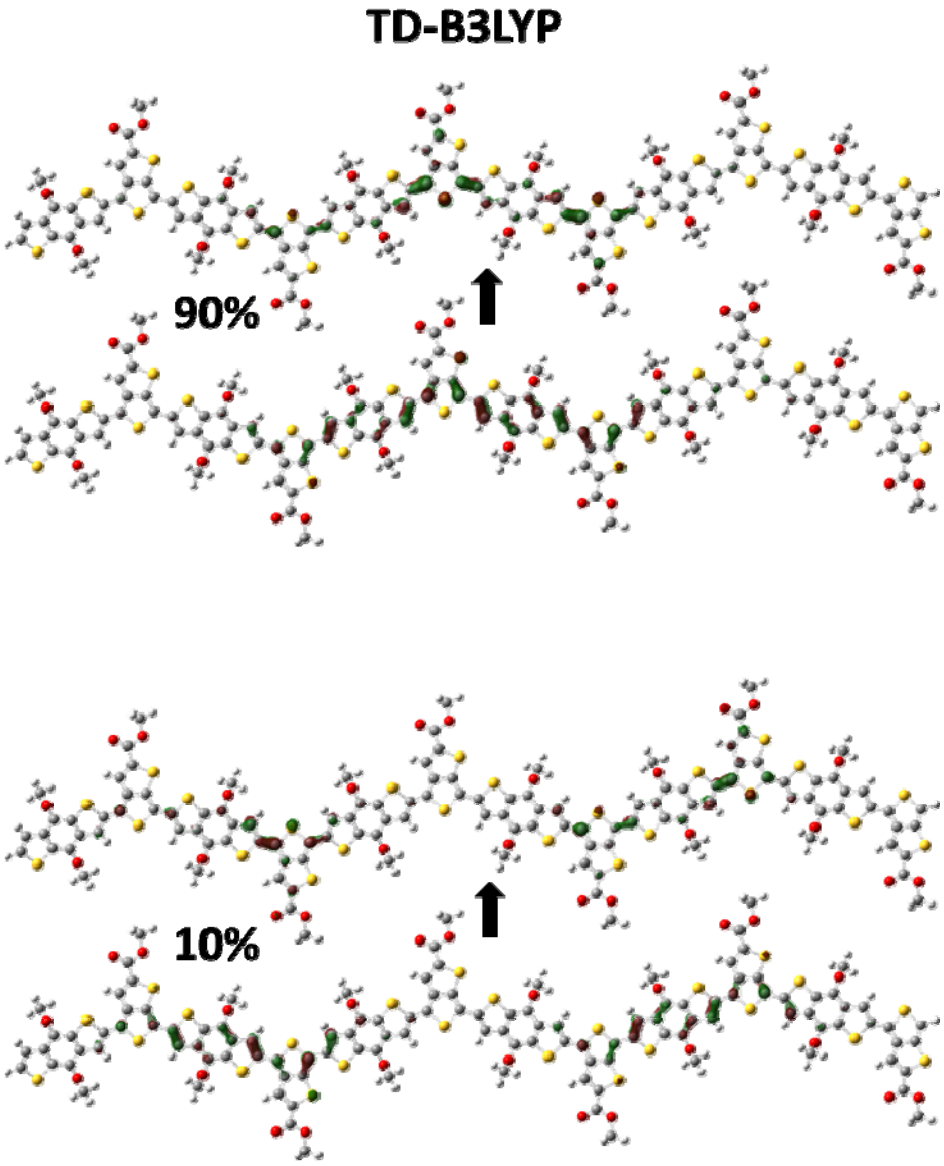

Figure S15 (a). Natural transition orbitals (isovalue surface 0.03 a.u.) for the $S_0 \rightarrow S_1$ excitation in the hexamer of PBDTTT-E at the TD-DFT level for B3LYP. Weights of the hole-particle contribution to the excitation also included.

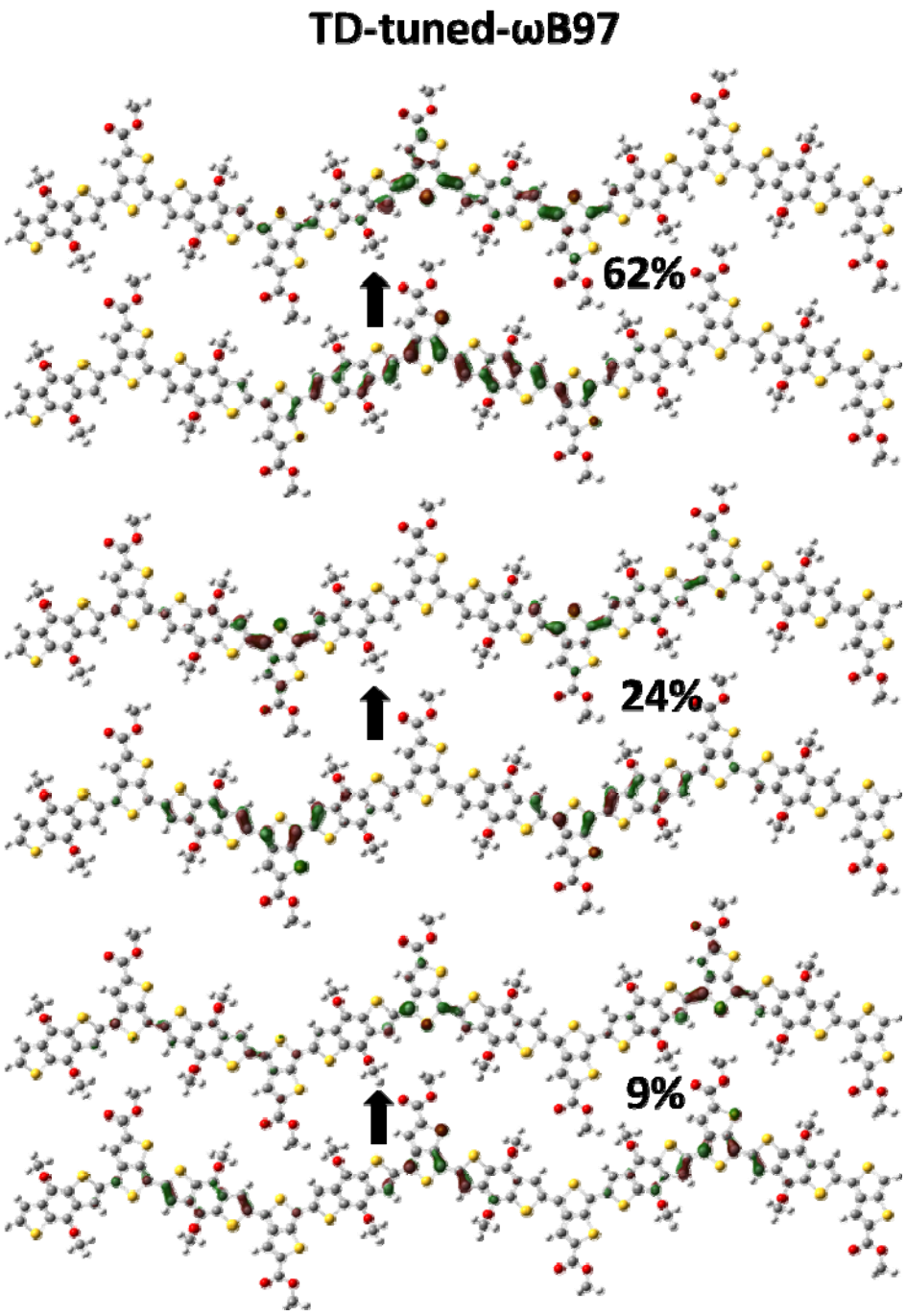

Figure S15 (b). Natural transition orbitals (isovalue surface 0.03 a.u.) for the $S_0 \rightarrow S_1$ excitation in the hexamer of PBDTTT-E at the TD-DFT level for tuned ωB97. Weights of the hole-particle contribution to the excitation also included.

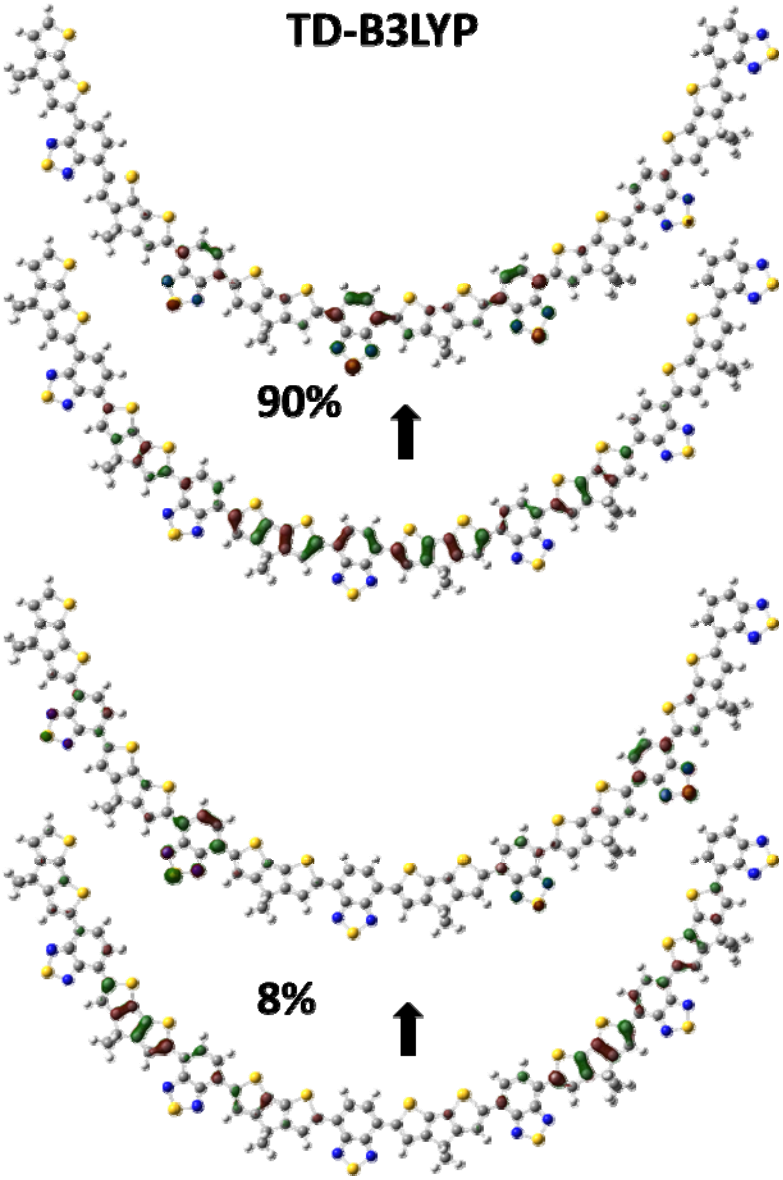

Figure S16 (a). Natural transition orbitals (isovalue surface 0.03 a.u.) for the $S_0 \rightarrow S_1$ excitation in the hexamer of PCPDTBT at the TD-DFT level for B3LYP. Weights of the hole-particle contribution to the excitation also included.

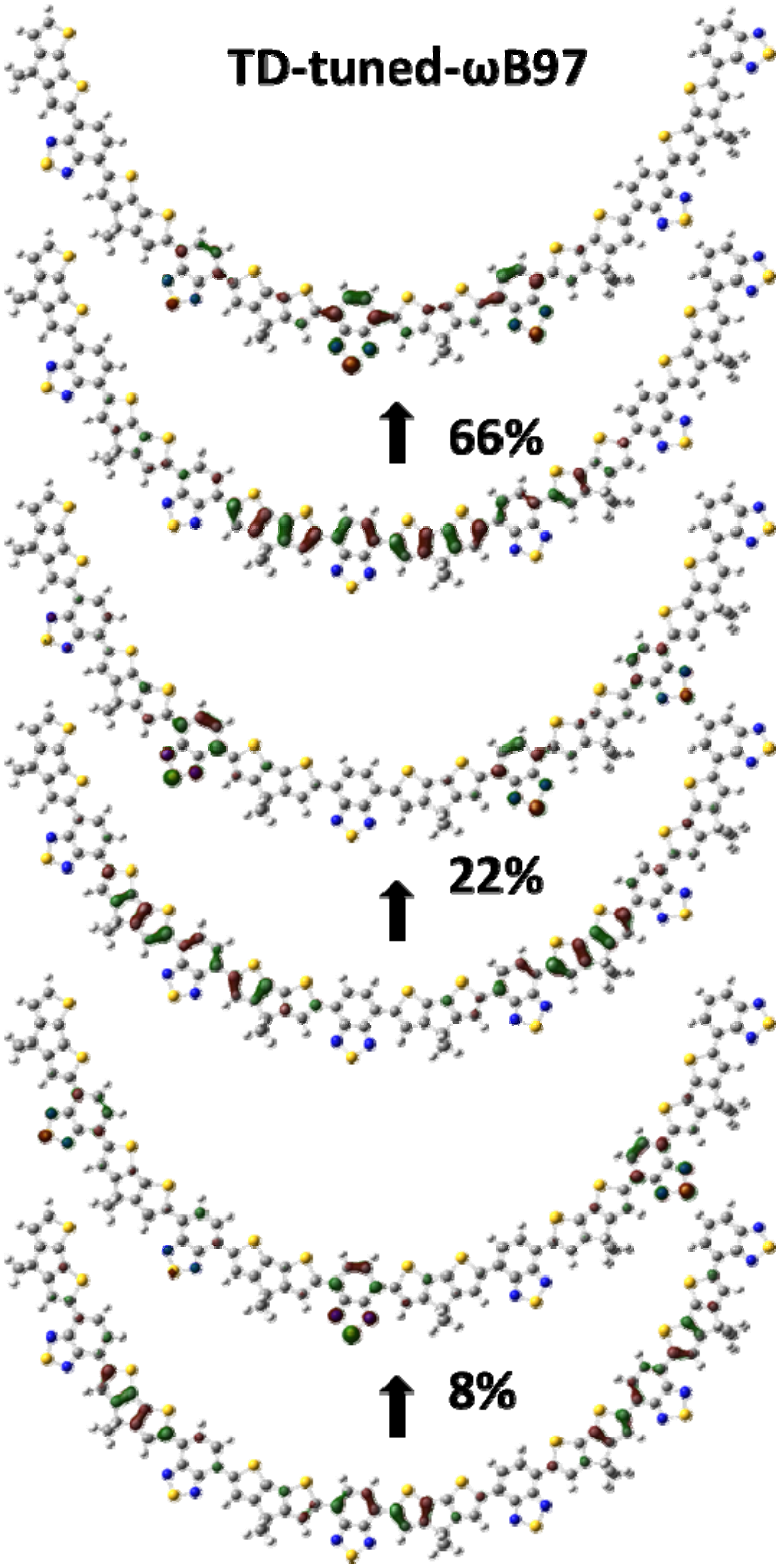

Figure S16 (b). Natural transition orbitals (isovalue surface 0.03 a.u.) for the $S_0 \rightarrow S_1$ excitation in the hexamer of PCPDTBT at the TD-DFT level for tuned ωB97. Weights of the hole-particle contribution to the excitation also included.

Table S2. TD-DFT $S_0 \rightarrow S_1$ transition energies (in eV) for the oligomers using the ωB97 (tuned and default ω) and B3LYP functionals.

n	1	2	3	4	5	6
B3LYP						
PBDTTPD	2.76	2.31	2.13	2.04	1.99	1.96
PBDTTT-C	2.61	2.11	1.89	1.78	1.72	1.68
PBDTTT-CF	2.59	2.15	1.93	1.83	1.76	1.75
PBDTTT-E	2.70	2.14	1.92	1.81	1.74	1.71
PCDTBT	2.15	1.93	1.86	1.83	-	-
PCPDTBT	2.31	1.73	1.49	1.36	1.29	1.24
Default ωB97						
PBDTTPD	3.72	3.16	2.99	2.93	2.87	2.85
PBDTTT-C	3.50	2.94	2.76	2.67	2.62	2.59
PBDTTT-CF	3.54	2.99	2.82	2.74	2.68	2.67
PBDTTT-E	3.54	2.93	2.77	2.68	2.63	2.60
PCDTBT	3.01	2.85	2.79	2.79	-	-
Tuned ωB97						
PBDTTPD	3.16	2.56	2.34	2.25	2.19	2.18
PBDTTT-C	3.01	2.33	2.08	1.97	1.90	1.88
PBDTTT-CF	3.03	2.38	2.14	2.03	1.95	1.95
PBDTTT-E	3.07	2.35	2.11	1.99	1.96	1.91
PCDTBT	2.53	2.24	2.18	2.18	-	-
PCPDTBT	2.81	2.00	1.68	1.53	1.44	1.39
PCPDTBT	3.24	2.54	2.34	2.24	2.19	2.16

Table S3. TD-DFT $S_0 \rightarrow S_1$ energies (in eV) at the polymer limit using linear (1/n) and exponential[5] extrapolation fits from the oligomer calculated data. The linear regression (Rsq) and parameter *a* (that describes how fast En saturates towards E_∞) are also included.

	Linear Fit (vs. 1/n)		Exponential Fit	
	E_∞	Rsq.	E_∞	*a*
B3LYP				
PBDTTPD	1.81	0.998	1.95	0.78
PBDTTT-C	1.51	0.996	1.67	0.73
PBDTTT-CF	1.58	0.992	1.72	0.70
PBDTTT-E	1.51	0.999	1.70	0.79
PCDTBT	1.72	1.000	1.82	1.04
PCPDTBT	1.05	0.996	1.23	0.73
Default ωB97				
PBDTTPD	2.66	0.998	2.86	0.99
PBDTTT-C	2.40	1.000	2.60	0.91
PBDTTT-CF	2.48	0.999	2.67	0.94
PBDTTT-E	2.40	0.998	2.62	0.99
PCDTBT	2.70	0.990	2.77	1.22
PCPDTBT	1.92	0.998	2.17	1.00
Tuned ωB97				
PBDTTPD	1.95	0.999	2.17	0.93
PBDTTT-C	1.63	0.999	1.87	0.88
PBDTTT-CF	1.70	0.999	1.93	0.87
PBDTTT-E	1.66	0.999	1.92	0.94
PCDTBT	2.03	0.979	2.17	1.61
PCPDTBT	1.11	0.999	1.38	0.81

References

1. H.-Y. Chen, J. Hou, S. Zhang, Y. Liang, G. Yang, Y. Yang, L. Yu, Y. Wu and G. Li, *Nat. Photonics*, 2009, **3**, 649-653.
2. N. Blouin, A. Michaud and M. Leclerc, *Adv. Mater.* , 2007, **19**, 2295-2300.
3. Y. Zhang, S. K. Hau, H.-L. Yip, Y. Sun, O. Acton and A. K.-Y. Jen, *Chem. Mater.*, 2010, **22**, 2696–2698.
4. D. Muhlbacher, M. Scharber, M. Morana, Z. G. Zhu, D. Waller, R. Gaudiana and C. Brabec, *Adv. Mater.* , 2006, **18**, 2884-+.
5. H. Meier, U. Stalmach and H. Kolshorn, *Acta Polym.*, 1997, **48**, 379-384.